arXiv:1512.04357v1 [hep-ph] 14 Dec 2015

The Diboson Excess: Experimental Situation and Classification of Explanations A Les Houches Pre-Proceeding

Johann Brehmer[1], Gustaaf Brooijmans[2], Giacomo Cacciapaglia[3], Adrian Carmona[4], R. Sekhar Chivukula[5], Antonio Delgado[6], Florian Goertz[4], JoAnne L. Hewett[7], Andrey Katz[4,8], Joachim Kopp[9], Kenneth Lane[10], Adam Martin[6], Kirtimaan Mohan[5], David M. Morse[11], Marco Nardecchia [12], Jose Miguel No[13], Alexandra Oliveira[14], Chris Pollard[15], Mariano Quiros[16], Thomas G. Rizzo[7], Jose Santiago[17], Veronica Sanz[13], Elizabeth H. Simmons[5], Jamie Tattersall[18]

[1] Institut für Theoretische Physik, Universität Heidelberg, Germany

[2] Nevis Laboratories, Columbia University, New York, NY 10027, USA

[3] Université de Lyon, F-69622 Lyon, France; Université Lyon 1, Villeurbanne and CNRS/IN2P3, UMR5822, Institut de Physique Nucléaire de Lyon, F-69622 Villeurbanne Cedex, France

[4] Theory Division, CERN, 1211 Geneva 23, Switzerland

[5] Department of Physics and Astronomy, Michigan State University, East Lansing, MI 48824, USA

[6] Department of Physics, University of Notre Dame, Notre Dame, IN 46556, USA

[7] SLAC National Accelerator Laboratory, Menlo Park, CA 94025, USA

[8] Université de Genève, Department of Theoretical Physics and Center for Astroparticle Physics (CAP), CH-1211 Geneva 4, Switzerland

[9] PRISMA Cluster of Excellence, 55099 Mainz, Germany, and Mainz Institute for Theoretical Physics, Johannes Gutenberg-Universität Mainz, 55099 Mainz, Germany

[10] Department of Physics, Boston University, Boston, MA 02215, USA

[11] Department of Physics, Northeastern University, Boston MA, USA

[12] DAMTP, University of Cambridge, Wilberforce Road, Cambridge CB3 0WA, United Kingdom

[13] Department of Physics and Astronomy, University of Sussex, BN1 9QH Brighton, UK

[14] Dipartimento di Fisica e Astronomia and INFN, Sezione di Padova, I-35131 Padova, Italy

[15] School of Physics and Astronomy, University of Glasgow, G12 8QQ Glasgow, UK

[16] Institut de Fisica d'Altes Energies (IFAE), The Barcelona Institute of Science and Technology (BIST), Institució Catalana de Recerca i Estudis Avançats (ICREA), Campus UAB, 08193 Barcelona, Spain, and ICTP-SAIFR & Instituto de Física Teórica, Universidade Estadual Paulista, São Paulo, Brazil

[17] CAFPE and Dpto Fisica Teorica y del Cosmos, University of Granada, E-18071, Granada, Spain

[18] Institut für Theoretische Teilchenphysik und Kosmologie, RWTH Aachen, Germany

March 3, 2022

CERN-PH-TH-2015-297

Abstract

We examine the 'diboson' excess at ~ 2 TeV seen by the LHC experiments in various channels. We provide a comparison of the excess significances as a function of the mass of the tentative resonance and give the signal cross sections needed to explain the excesses. We also present a survey of available theoretical explanations of the resonance, classified in three main approaches. Beyond that, we discuss methods to verify the anomaly, determining the major properties of the various surpluses and exploring how different models can be discriminated. Finally, we give a tabular summary of the numerous explanations, presenting their main phenomenological features.

Contents

1 Introduction **3**

2 Experimental Results **3**
2.1 Results Considered 3
2.2 Comparison of Excess Significances 4
2.3 Signal Cross Sections 4

3 Theoretical Interpretation **6**
3.1 Simplified Model Description of an s-channel Resonance 7
3.2 Strongly Coupled Dynamics 10
3.2.1 Drell-Yan production: Spin-one resonances 10
3.2.2 Gluon-fusion production: Spin-zero and -two resonances 12
3.3 Enlarged Gauge Group 14
3.3.1 Left-right symmetry 15
3.3.2 Other models with extended gauge groups 18
3.4 Extended Higgs Sectors 19

4 Phenomenology for Run 2 **21**
4.1 Resonance Production and Decay Modes 22
4.2 Proposed Run 2 Studies 23
4.3 Precision Measurements 25

5 Overview of the Models **25**

6 Conclusions **26**

1 Introduction

The LHC has pushed particle physics to a new energy frontier. After the first successful run at 8 TeV when the Higgs was discovered, the machine restarted this year with collisions at 13 TeV. This new run will serve to study the Higgs properties to a much better precision that we already know but it will also confirm or disregard some possible new physics signals coming from excesses in different channels with respect to the expected number of events.

Several of those excesses come from the search for heavy resonances around 2 TeV, and the fact that they are in several channels and appearing in both ATLAS and CMS analyses has driven lots of attention in the community. The possible signal could be interpreted as a heavy bosonic resonance decaying into two SM electroweak vector bosons. There have been many theoretical papers trying to explain the signal within different models and there have also been some attempts to combine the different channels into one single significance plot.

The aim of this paper is to summarize in a single document both the experimental and the theoretical situation of the 'diboson' excess in preparation for the data coming from the LHC 13 TeV run. Should the excess be confirmed the reader could easily use this document as a first point to check which one of the possible approaches are more likely to be able to explain not only the existing excesses but any other that may come in different channels. By having a comprehensive analysis of the different ideas we hope to present a clear explanation of the situation.

The paper is organized as follows. The different experimental signals are summarized in section 2. Section 3 contains a summary of the different possible resonances that could explain the excesses. We will discuss the phenomenology for run 2 in section 4, section 5 is devoted to an overview of the different models and finally our conclusions are presented in section 6.

2 Experimental Results

The primary reason the "diboson" excess is of interest is that there are excesses in multiple analyses searching for heavy resonances in the region between 1.5 and 2.5 TeV. These excesses are not limited to the diboson decay channels, so any multi-channel combination would require significant assumptions about the underlying model, leading to an inherent bias in the ensuing conclusions. Instead, the results are presented in two ways: a) a comparison of the excesses as a function of mass in units of standard deviations, and b) a comparison of the signal cross sections needed to lead to these excesses, also as a function of resonance mass. As this was finalized, an informal ATLAS–CMS combination of individual channels was released [1].

2.1 Results Considered

The following experimental results are considered:

- Diboson resonance searches that do not include Higgs bosons: ATLAS and CMS searches in the all-hadronic [2, 3], $\ell\nu$ (where ℓ denotes an electron or muon) plus hadrons [4, 5] and $\ell\ell$ plus hadrons [5, 6] final states;
- ATLAS and CMS WH resonances searches in the $\ell\nu b\bar{b}$ final state [7, 8];
- An ATLAS ZH resonance search in the $\ell\ell b\bar{b}$ and $\nu\nu b\bar{b}$ final states [7];
- A CMS WH and ZH resonance search in the all-hadronic final state [9];
- A CMS ZH resonance search in the $\tau\tau$ plus hadrons final state [10];
- A CMS W_R boson search in the $\ell\ell$ plus hadrons [11];
- ATLAS and CMS searches for dijet resonances [12, 13];
- ATLAS and CMS dilepton resonance searches [14, 15].

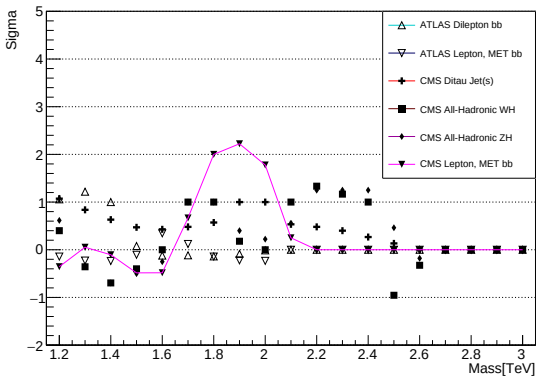
2.2 Comparison of Excess Significances

To extract this information, the limit plots from the different results are digitized: the observed, expected, and expected plus one and two σ limits are recorded for resonance mass values between 1.2 and 3.0 TeV in 100 GeV steps. To calculate the excesses in units of σ, simple approximations are used: if the excess lies between one and two σ, a linear interpolation between the expected plus one and two σ values is performed; if the excess is less than one (or larger than two) σ, a linear interpolation (extrapolation) using the expected and expected plus two σ values is performed. This method attempts to take into account that the slope of a gaussian is steeper between one and two σ than elsewhere. While the expected limit distribution for a given resonance mass is not necessarily gaussian, for this comparison the approximation is of sufficient quality. The results are shown in Fig. 1 separately for decays including a Higgs boson, and decays without Higgs bosons, compatible with either a charged or neutral resonance. For decays with a Higgs boson, only the CMS $\ell\nu b\bar{b}$ search shows a significant excess, between 1.7 and 2.1 TeV. For charged and neutral resonances, overlapping significant excesses are found in the region between 1.8 and 2.0 TeV.

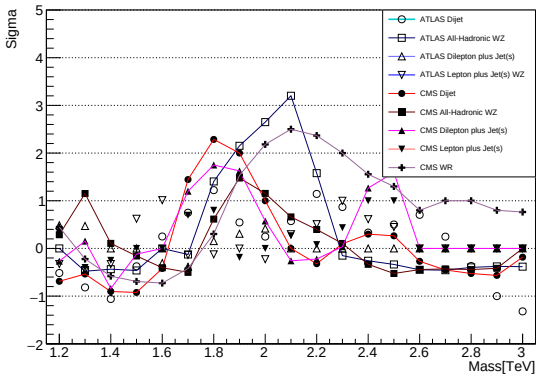
2.3 Signal Cross Sections

The signal cross sections needed to produce the observed excesses are calculated based on the observed, expected, and expected plus one and two σ limits. For the dijet resonances, the limit plots include an acceptance factor, and the results are divided by the acceptance factor for W' bosons given by ATLAS. (Acceptance values for W' bosons from CMS were not found, but for other signals the values for ATLAS and CMS agree well.) For the CMS dilepton resonance search, the limit is given as a ratio to the Z boson cross section times branching ratio to electrons and muons. To convert to fb, this is assumed to be equal to 2 nb.

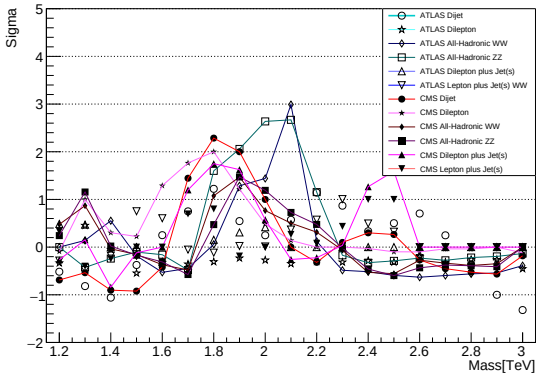
To evaluate the signal cross sections, each mass point is initially treated as a single counting experiment. Signal and background are each assumed to be affected by a single uncertainty, and these uncertainties, as well as the signal and background cross sections are adjusted to reproduce the values obtained from the limit plots. The limits are calculated using the CL_s method with the profile likelihood test statistic (as done by the



(a)



(b)



(c)

Figure 1: Comparison of the excess magnitudes in high mass resonance searches in units of standard deviations for (a) decays including a Higgs boson, and (B,c) decays without Higgs bosons compatible with a charged (b) and a neutral (c) resonance. Channels which exceed a 1.5 σ excess are shown with lines, others without.

experiments). The background uncertainty drives the differences between the expected and expected plus one and two σ limits. In this simplified approach, it is often impossible to make it small enough to match the values in the limit plots. Tests indicate this has a negligible impact on the signal cross section needed to reproduce the excess. To account for the use of the full invariant mass distribution by the experiments, the obtained signal cross sections are multiplied by a factor 0.7. This is obtained from an ATLAS study comparing the sensitivity to dilepton resonances using the full invariant mass distribution with that obtained from counting experiments in narrow mass windows [16]. The resulting signal cross sections agree reasonably well with those obtained when using the number of observed events, signal efficiencies and acceptances in the few cases where this information is available. An uncertainty of 30% should cover the limitations of the method used. The results are shown in Figure 2.

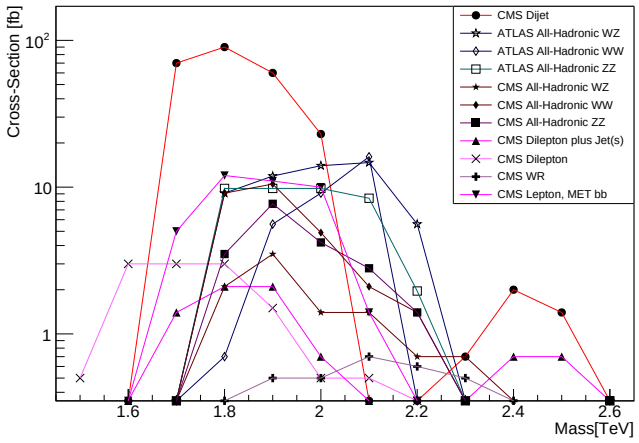


Figure 2: Estimated signal cross sections for searches with excesses larger than 1.5 σ.

3 Theoretical Interpretation

In this section, we summarize the major approaches for explaining the diboson excess in terms of extensions of the Standard Model. Most of these involve production and decay of a single, relatively narrow s-channel resonance. We begin by using a simplified model of such a resonance to convert an estimated signal cross-section into model-independent *lower* bounds on the branching ratios for the resonance that correspond to the production and decay modes. For estimated cross-sections of 1 - 100 fb, we find that the vector-boson fusion production mode must be subdominant. Next, we turn to a discussion of the three main classes of physics beyond the standard model that have been invoked to explain the diboson excess, namely, strongly-coupled scenarios such as composite Higgs models, modifications of the Standard Model (SM) gauge group, and extensions of the scalar sector. More exotic solutions beyond this classification will be summarized in Section 5.

3.1 Simplified Model Description of an s-channel Resonance

There are many Beyond the Standard Model possibilities that may explain the diboson excesses discussed in this work. In most cases, the excess arises from the production and decay of a single, relatively narrow, s-channel resonance. In this context, a simplified model of the resonance allows us to convert any estimated signal cross section into model-independent constraints on the properties of the resonance. In particular, if resonance production occurs dominantly through a single process, we can obtain model-independent *lower* bounds on the product of the branching ratios corresponding to production and decay. Any resonance proposed to explain an excess in pairs of final-state weak bosons can certainly be produced via vector-boson fusion and can potentially be produced through $q\bar{q}$ annhilation and/or gluon fusion as well. The simplified model analysis shows immediately that, in order to explain the size of the excesses discussed here, vector boson fusion cannot be the dominant production mechanism.

The tree-level partonic production cross-section for an arbitrary s-channel resonance at the LHC can be written [17, 18]

$$\hat{\sigma}_{ij\to R\to xy}(\hat{s}) = 16\pi\cdot\mathcal{N}\cdot\frac{\Gamma(R\to i+j)\cdot\Gamma(R\to x+y)}{(\hat{s}-m_R^2)^2+m_R^2\Gamma_R^2}\ , \tag{1}$$

where $\mathcal{N}$ is a ratio of spin and color counting factors

$$\mathcal{N} = \frac{N_{S_R}}{N_{S_i}N_{S_j}}\cdot\frac{C_R}{C_iC_j}, \tag{2}$$

where N_S and C count the number of spin- and color-states for initial state partons i and j and for the resonance R. In the narrow-width approximation one can simplify this further using.

$$\frac{1}{(\hat{s}-m_R^2)^2+m_R^2\Gamma_R^2} \approx \frac{\pi}{m_R\Gamma_R}\delta(\hat{s}-m_R^2)\ . \tag{3}$$

Assuming that one production mechanism ($x+y\to R$), dominates, we can write down the signal cross-section for pp-collisions as follows.

$$\sigma_R(pp\to x+y) = \int_{s_{min}}^{s_{max}} d\hat{s}\,\hat{\sigma}(\hat{s})\cdot\left[\frac{dL^{ij}}{d\hat{s}}\right]\ , \tag{4}$$

and hence

$$\sigma_R(pp\to x+y) = 16\pi^2\mathcal{N}\frac{\Gamma_R}{m_R}BR(R\to i+j)\cdot BR(R\to x+y)\left[\frac{dL^{ij}}{d\hat{s}}\right]_{\hat{s}=m_R^2}\ . \tag{5}$$

Here $\frac{dL^{ij}}{d\hat{s}}$ corresponds to the luminosity function for the ij combination of partons[1].

Using this expression, we can immediately derive model-independent bounds on the branching ratios of the resonance [20].

[1] We calculate these parton luminosities using the `CTEQ6L1` [19] parton density functions, setting the factorization scale $q^2=\sqrt{\hat{s}}$.

To illustrate this point, consider the possibility of a charged spin-one color-neutral vector resonance – a technirho or a W' – decaying to $W^{\pm}Z$. Such an object can be produced either via vector boson fusion or via $q\bar{q}$ (in this case primarily $u\bar{d}$ or $d\bar{u}$) annihilation. For vector boson fusion production, we see that the signal cross section (in this simplified model) is determined entirely by $BR(R \to WZ)$, which is bounded from above by 1; for $q\bar{q}$ production, on the other hand, the signal cross section is determined entirely by $BR(R \to q\bar{q}) \cdot BR(R \to WZ)$, which is bounded from above by 1/4.

In Figures 3 and 4 we plot the *lower bounds* for the appropriate branching ratios corresponding to vector boson fusion (calculated in the effective W approximation [21]) and $q\bar{q}$ annihilation production assuming $\Gamma_R/m_R = 0.1$ and for signal cross sections of 1, 10, and 100 fb – of order the excesses described in this work. Looking at Figure 3, we see that the lower bounds on $BR(R \to WZ)$ exceed 1; therefore, vector boson fusion must be only a subdominant production mode for any resonance responsible for the observed diboson excess. In contrast, from Figure 4 we see that $q\bar{q}$ annhilation can be consistent with the observed excesses so long as the product of the branching ratios to WZ and $q\bar{q}$ lie within the shaded region.

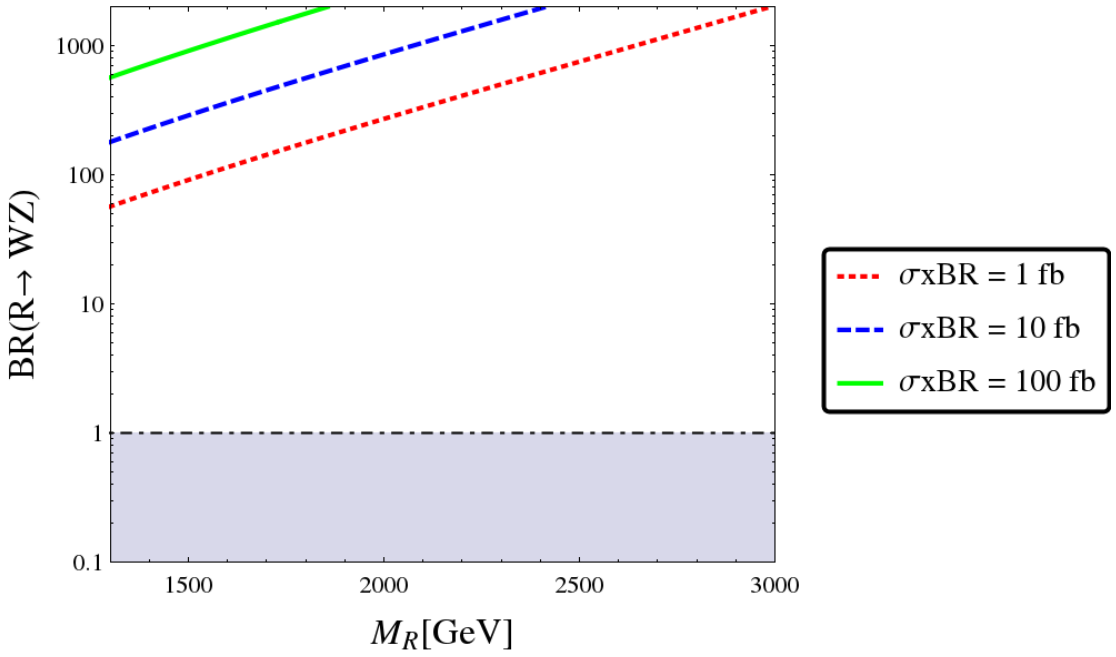


Figure 3: Lower bounds on branching ratio $BR(R \to WZ)$ assuming production of an s-channel resonance R with $\Gamma_R/m_R = 0.1$ via vector boson fusion, shown for three different values of $\sigma \times BR$. Since the lower bounds exceed the value 1, the VBF process cannot be the dominant production mode for a resonance R that is causing the observed diboson excess.

This analysis can be easily extended to other resonances, and corrected for geometrical acceptance and efficiency, but the general conclusions remain the same [20].

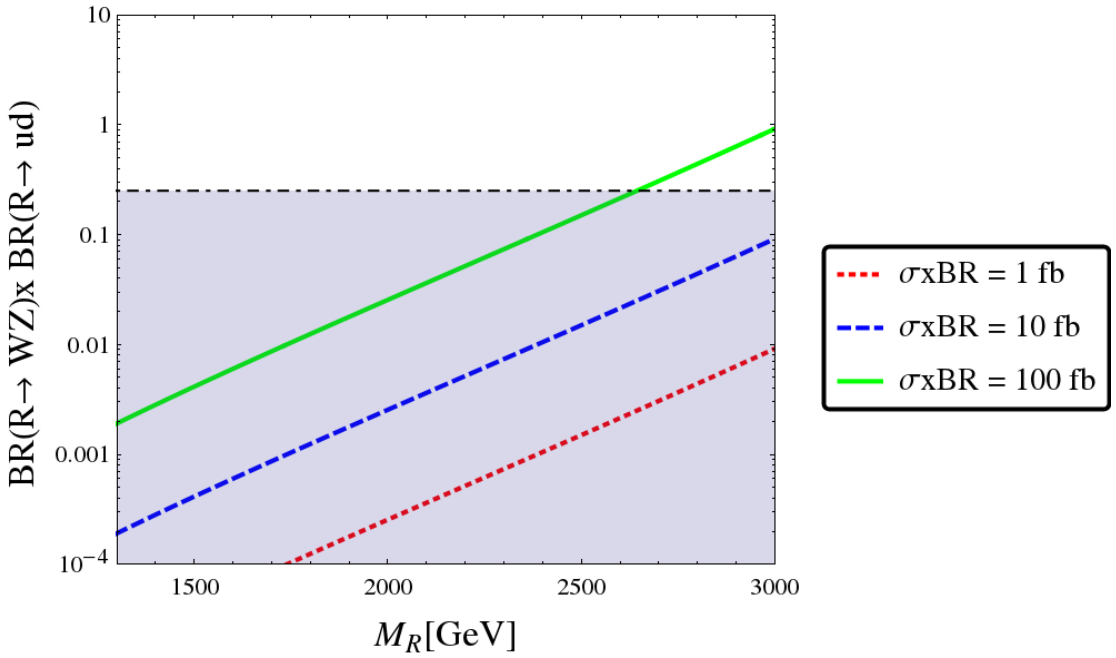


Figure 4: Lower bounds on the product of branching ratios $[BR(R \to WZ) \times BR(R \to ud)]$ for production of an s-channel resonance R with $\Gamma_R/m_R = 0.1$ via quark anti-quark annihilation, for three different values of $\sigma \times BR$. The portions of the curves lying within the shaded region correspond to values of the product of branching ratios for which a $q\bar{q}$-produced resonance could be consistent with the observed diboson excess.

3.2 Strongly Coupled Dynamics

Models of strongly coupled dynamics in all their different incarnations [22–29] are among the most popular solutions to the hierarchy problem. In general, in these models, the quadratic ultra-violet (UV) sensitivity of the Higgs mass is saturated at some scale $\Lambda \sim \mathcal{O}(\text{TeV})$, before the new strong interaction starts to be resolved. In addition, the Higgs boson can be expected to be lighter if it is identified with the pseudo Nambu-Goldstone boson (pNGB) associated to the spontaneous symmetry breaking of some global symmetry of the strong sector. This is for instance the case of Composite Higgs models, or their holographic duals, where the Higgs arises as the pNGB of some global symmetry of the strong dynamics [30–32], or some walking Technicolor scenarios, where the Higgs is thought to be the dilaton appearing from the breaking of the (approximate) conformal symmetry by the strong dynamics [33–37].

The above scale Λ is in general populated by resonances, bound states of UV fields which would couple to the Higgs and massive vector bosons, analogous to the coupling of the QCD $\rho(770)$ meson to pions. In the following we will describe proposals to explain the diboson resonance in terms of heavy composite states from such a scenario, exploring different options in terms of quantum numbers, namely $J^{CP} = 1^{--}$, 0^{++} and 2^{++}, as well as their couplings to other SM particles besides massive bosons. Note that the production mechanisms for spin-one resonances are via Drell-Yan and (more suppressed) vector boson fusion (VBF), whereas the spin-zero and -two resonances can be produced via gluon fusion.

3.2.1 Drell-Yan production: Spin-one resonances

Typically, in Composite Higgs models one considers the lightest of these states to be a spin-one resonance ρ_μ with vector couplings to the quarks, and in some works a second axi-vector resonance a_μ is also considered. This expectation comes from experience from QCD, as well as dual pictures of Composite Higgs where the SM gauge fields are propagate in the bulk of an extra-dimension. In general, if the UV strong sector would contain light fermions, one would expect these to form bound states with quantum numbers 1^{--} which could be at the bottom of the resonance sector. These spin-one resonances are expected to feature sizeable couplings with the longitudinal components of the SM weak bosons in analogy to the QCD case, where $g_{\rho\pi\pi} \sim g_\rho \gg 1$ [38], becoming therefore natural candidates to account for the diboson anomaly observed at the LHC.

Because of the aforementioned reasons, it is not surprising that the first models of strongly coupled dynamics trying to address the diboson anomaly that appeared relied on the effect of isospin triplet vector resonances $\rho^\pm, \rho^3$ [39–46], which are mostly produced by Drell-Yan (DY), since the $\mathcal{O}(m_W^2/m_\rho^2)$ suppression in their couplings to the transverse polarizations of the SM gauge bosons make their VBF production sub-leading. This is true since, in addition to the $\mathcal{O}(\alpha_W^2)$ suppression of the latter, even in the case of elementary fermions, the coupling to fermions induced by the $\rho - V$ gauge mixing is expected to be $\sim g^2/g_\rho$, which is $\mathcal{O}(v^2/f_\rho^2)$ bigger than the one involved in VBF,

where $f_\rho \sim m_\rho/g_\rho \gg v$. [2] Another common feature of these models is the absence of ZZ production, being the decay $\rho^0 \to ZZ$ isospin violating. Therefore, the anomaly in such channel can be only explained via leakage from the other channels, WW and WZ, which is expected to be large taking into account the ATLAS mass windows defined for the W/Z discrimination.

From the theoretical point of view, one of the first concerns arising in these scenarios is the problematic interplay of such a *light* resonance with electroweak precision tests (EWPT). The main idea is that tree level ρ contribution to the S parameter will be $\gtrsim 4\pi v^2/m_\rho^2$. Taking $m_\rho \sim 2\,\text{TeV}$ and making numbers, it can be readily seen that if one considers the electroweak fit [47] at face value, these resonances will be well excluded. However, since they are expected to be part of a more complete theory of electroweak symmetry breaking (EWSB), where new contributions to the oblique parameters are expected, this naive counting has to be taken with a grain of salt. First of all, in technicolor theories or general composite models where the second Weinberg sum rule can be relaxed [48], the contribution of the vector resonance to the S parameter can be partially cancelled by the one from its axial counterpart

$$S \simeq 4\pi \frac{v^2}{f_\rho^2 + f_a^2}\left(\frac{f_\rho^2}{m_\rho^2} - \frac{f_a^2}{m_a^2}\right), \tag{6}$$

provided that $f_\rho/f_a \sim m_\rho/m_a$, where $m_a \sim g_a f_a$. This is actually the case in some technicolor scenarios exhibiting a near conformal behaviour, where nearly degenerate vector and axial resonances are expected [49–53]. Such a cancellation has been argued for instance in [39, 43, 44]. Moreoever, in the case of *regular* composite Higgs models, the presence of anomalously light top partners is typically required by naturalness [48, 54–58], which can lead via radiative corrections to a more than welcome positive contribution to the T parameter [59], taking into account the strong correlation between both observables. [3] On the other hand, a departure from the universal case (having e.g. different ρ couplings to light quarks and leptons) opens an extra (although limited) room for improvement in the electroweak fit. This is the case e.g. in [42], where suppressed lepton couplings were required to accommodate dilepton bounds, even though the agreement with EWPT arised mainly from a small breaking of custodial symmetry [60, 61]. Finally, UV corrections at the cutoff scale may also be important [62].

Another potential issue arising in models of composite Higgs, where the fermion masses are generated by partial compositeness, is that the natural presence of light partners will most likely substantially change the simple picture presented until now. Since these colored fermionic states Q will typically have masses $m_Q \ll m_\rho \sim g_\rho f_\rho$, and will feature sizable couplings to the vector resonances $g_{\rho QQ} \sim g_\rho$, the diboson branching ratios will be diluted by a much larger total width, if the decay channel $\rho \to Q\bar{Q}$ opens and they can be pair produced [63–66]. Even in the case when only single production of top partners is allowed, since a large degree of compositeness is expected for the top

[2] Note that in the limit of very large g_ρ, VBF can become relevant. This was explored e.g. in Ref. [44].

[3] However, their presence may affect the setups at hand. See discussion below.

chiralities, the couplings $g_{\rho tQ}$ involved will not be negligible, and their presence will complicate the analyses presented hitherto. However, the presence of anomalously light top partners is not compulsory in natural models [67–71] and it is always possible to avoid them at the price of increasing the fine tuning. Alleviating these problems is among the motivations of [45], where the vector resonances at hand are embedded into a twin Higgs framework that assures the absence of light fermionic partners. Another related issue is that the sizable degree of compositeness $\epsilon^t_{L,R}$ required to generate the top mass can make $g_{\rho t_{L,R} t_{L,R}} \sim g_\rho \epsilon^t_{L,R} \epsilon^t_{L,R}$ large enough to render the channels $\rho^0 \to t\bar{t}$ and $\rho^+ \to t\bar{b}$ competitive with respect to the diboson ones. [4] To a lesser extent, this is also the case for $\rho^0 \to b\bar{b}$, which will also fed into the dijets searches. However, at the end of the day, these constraints turn out to be relevant only for large values of g_ρ and ϵ^t_L [45], or for moderate values of g_ρ and large mixing angles ϵ^q_L [42], when the dijet branching ratio becomes important.

To illustrate some of these issues and the interplay between the different constraints we show in Figures 5 and 6 the viable parameter space for a couple of particular examples, taken from Refs. [42, 45]. In the first case, the relatively small value of $g_\rho = 0.75$ preferred by EWPT in that model, together with the sizable couplings to light quarks $g_q \sim g_\rho (\epsilon^q_L)^2$ required to make DY production significant, make impossible to neglect dijet or $t\bar{t}$ searches, as can be readily seen by looking at Figure 5. However, in the case of models where $T = 0$ at the tree level and g_ρ is expected to be significantly larger, like the ones illustrated in Figure 6, the most relevant direct constraints arise essentially from dilepton searches when g/g^2_ρ starts to become relevant.

3.2.2 Gluon-fusion production: Spin-zero and -two resonances

As we discussed, in the usual Composite Higgs scenarios one needs a baryonic resonance (the top-partner) among the low-lying states to trigger EWSB. This in turn indicates that the UV theory would exhibit a chiral symmetry in analogy to QCD, leading to the expectation that spin-one states composed by light UV quarks would be relatively light. In QCD-like models, as well as in extra-dimensional models, the 1^{--} resonances are lighter than the 0^{++} and 2^{++} bound states, hence their phenomenology is more relevant.

But this is not the only scenario for a new strong sector in Composite Higgs. An alternative explanation would be that EWSB is triggered by other means not involving top-partners, e.g. via a see-saw mechanism [72]. In this case, the structure of the UV theory can differ from the usual Composite Higgs models, leading to a resonance structure distinctly different from the cases discussed in the previous section.

Such a scenario in terms of a pure-gauge UV completion has been proposed in Ref. [73]. In this proposal, the lightest states are glueballs, bound states formed by gauge fields. The glueball spectrum has been studied in the lattice [74] and one finds

[4] Smaller mixing angles ϵ^t_L for the third generation are expected in twin Higgs models [45] and also in the UV completion of [42], even though the required values used in the latter to explain the excess without disagreement with other searches seem a bit on the edge.

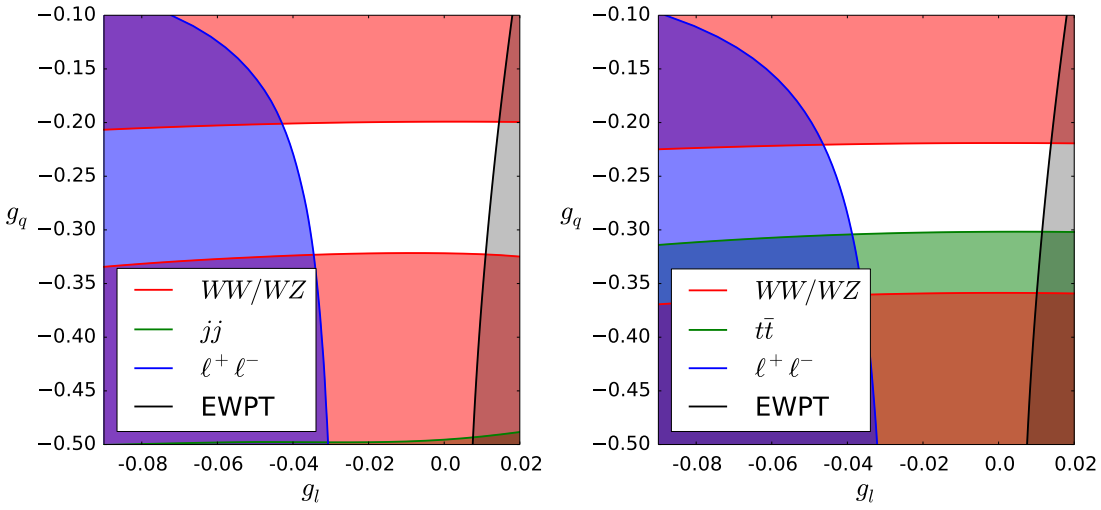


Figure 5: Constraints on the parameter space of the model in Ref. [42] from the diboson signal, $t\bar{t}$, dijet, $\ell^+\ell^-$ and EWPT. The colored areas correspond to the region excluded by the different bounds. Here, $m_\rho = 1.8$ TeV, $g_\rho = 0.75$ and $g_\rho \epsilon_L^{q_3 2} = 0.3$, whereas $g_\rho \epsilon_R^{t\,2} = 0.3\,(0.5)$ for the left (right) plot. See Ref. [42] for more details.

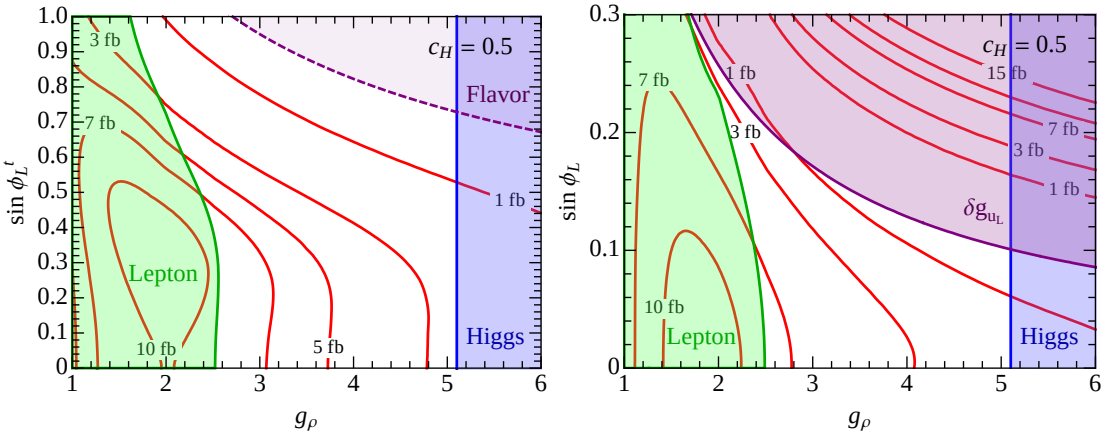


Figure 6: Constraints on the parameter space of the two-site model in Ref. [45] for $m_\rho = 2$ TeV. In the left-hand side plot, all leptons and light quarks have been assumed to be elementary and $\sin\phi_L^t \equiv \epsilon_L^t$. In the right-hand side plot, $\sin\phi_L \equiv \epsilon_L^{q_1} \equiv \epsilon_L^{q_2}$, whereas ϵ_L^t has been fixed to 0.4. See Ref. [45] for more details.

that typically the 0^{++} and 2^{++} states dominate the phenomenology. In [73] it was argued that the behaviour of these glueballs should resemble the radion and Kaluza-Klein graviton states in extra-dimensional theories, with a notable difference that in the glueball theory the spin-one states are no lighter than the massive graviton, hence the strong constraints on the electroweak precision parameters S and T (discussed in the

previous section) do not apply in this scenario. The glueballs are singlets under the SM interactions and would be produced via gluon fusion, with preferential decays to other (lighter) composite states, namely the Higgs, longitudinal W and Z bosons and possibly the top. As they are initiated by gluons, the production of these resonances would increase substantially in Run2. See Table 1 for a summary of the experimental signatures of this scenario and Fig. 7 for a plot summarizing the cross section for the distinct spin-two case.

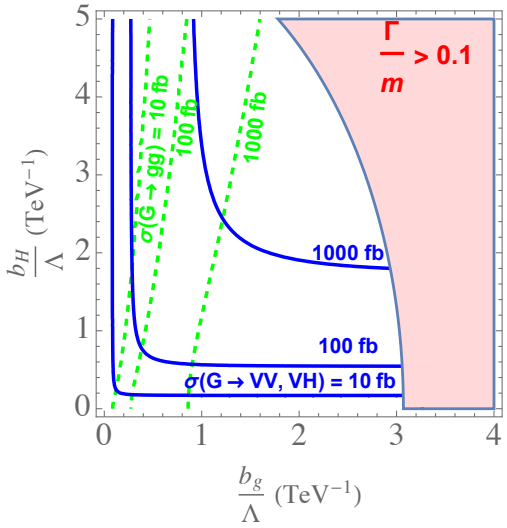


Figure 7: Total cross sections at LHC8 for 2 TeV spin-two states in the HV and VV channels and digluon final state as a function of the coupling of the glueball to gluons and Higgs degrees of freedom. Cross sections do not include efficiencies to cuts, and the shaded region correspond to a width above 10% of the mass [73].

Finally, let us mention that in Ref. [75], scalar glueballs were discussed in a scenario with a UV completion involving scalars and unrelated to Composite Higgs, where one would not expect preferential couplings to massive particles. For this reason, the phenomenology of this scenario is different from the glueballs related to Composite Higgs, as there are no specific predictions of branching ratios.

3.3 Enlarged Gauge Group

The decay of a heavy resonance to gauge bosons can arise naturally in scenarios with an enlarged non-Abelian gauge sector. In such models the excesses can be interpreted as a new heavy gauge boson decaying through a triple gauge boson vertex. A heavy neutral gauge boson is typically called Z', while a heavy charged gauge boson is usually denoted by W'.

The proposed explanations have some common phenomenological features:

- Quarks are charged under the extended gauge groups, so the heavy gauge bosons are produced copiously via the Drell-Yan process. In fact, the W' or Z' production cross section can easily reach a few hundred fb for a mass around 2 TeV and weak gauge couplings.

- This directly implies that the W' or Z' decays into qq', leading to potential signatures in dijet, tb and $t\bar{t}$ final states. Depending on the model there may also be leptonic decays, but these are strongly constrained from $\ell^+\ell^-$ and $\ell\nu$ searches.

- To explain the diboson excess, couplings to WZ, WW, or ZZ states are necessary. The equivalence theorem [76] then suggests $W' \to Wh$ or $Z' \to Zh$ decay modes of similar size.

For concreteness, we will now focus on one particular scenario, the left-right symmetric model with gauge group $SU(2)_L \times SU(2)_R \times U(1)_{B-L}$, in which the excess is explained in terms of the righthanded W_R boson decaying to WZ pairs. We will then give an overview of other proposals.

3.3.1 Left-right symmetry

In the context of the diboson excess at the LHC, the most studied framework with an enlarged gauge sector is the left-right symmetric model based on the gauge group $SU(2)_L \times SU(2)_R \times U(1)_{B-L}$ [77–82]. Recent studies in the context of the diboson anomaly have been presented in Refs. [83–105] (see also Ref. [106] for a study utilizing a W' toy model, which can be considered a phenomenological reduction of the full left-right symmetric model). In models of this type, right-handed fermions are collated into doublets of the new gauge group $SU(2)_R$ in the same way as their left-handed counterparts are members of $SU(2)_L$ doublets. The model can thus restore parity as an exact (but spontaneously broken) symmetry of nature.

At a scale $\gg 100$ GeV, $SU(2)_R \times U(1)_{B-L}$ is spontaneously broken to $U(1)_Y$, with the most popular breaking mechanism involving a triplet Higgs field Δ_R with quantum numbers $(1, 3, 2)$ under $SU(2)_L \times SU(2)_R \times U(1)_{B-L}$ (see Fig. 8). The *vev* of Δ_R gives mass to the $SU(2)_R$ gauge bosons W_R, Z_R. At the electroweak scale, a Higgs bidoublet $\Phi \sim (2, 2, 0)$ then breaks the residual $SU(2)_L \times U(1)_Y$ to $U(1)_{\rm em}$, also endows the $SU(2)_L$ gauge bosons W_L, Z_L with masses, and leads to a small mixing between W_L, W_R as well as between Z_L, Z_R. We thus obtain two physical charged gauge bosons $W \simeq W_L$ and $W' \simeq W_R$, with $m_W \ll m_{W'}$. Similarly, the physical neutral gauge boson states Z and Z' satisfy $m_Z \ll m_{Z'}$. This breaking scheme of the left-right symmetric gauge group has the additional benefit that the vev of Δ_R generates a Majorana mass term for the right handed neutrinos (which are automatically part of the model thanks to the doublet structure of right handed fermions).

At the LHC, W' bosons can be efficiently produced through their coupling to right-handed quarks. They subsequently decay either to quarks (leading to dijet and tb resonance signatures), via $W' \to WZ$ (explaining the diboson signature), or into Wh.

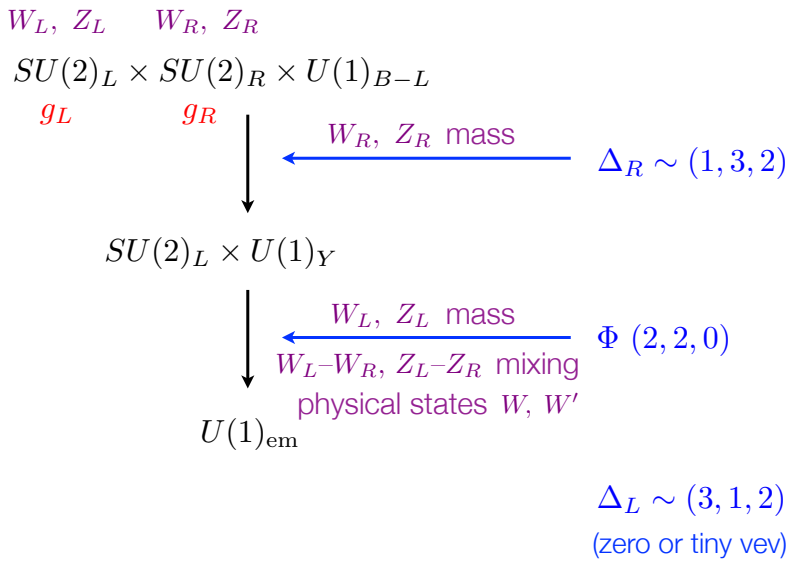


Figure 8: A typical breaking scheme for the left-right symmetric gauge group $SU(2)_L \times SU(2)_R \times U(1)_{B-L}$.

The latter decay modes are generated by the small mixing between W_L and W_R. Depending on the mass of the right-handed neutrinos, there may also be a $W' \to \ell N_R$ decay [83, 86, 92, 94, 95, 97–100, 103, 104]. W' decays into the additional Higgs bosons of the extended scalar sector [92], or into new fermion multiplets [88, 90, 93, 98, 99] have also been discussed. Finally, the authors of Ref. [107] have analysed three-body and four-body decays.

It turns out that this right-handed W' boson can explain the diboson excess while being consistent with all other current limits from LHC searches. For good agreement with data, the following conditions must be satisfied (see Fig. 9):

- The W' boson must have a mass $m_{W'} \sim 1.8 \ldots 2.0$ TeV.
- The $SU(2)_R$ coupling constant g_R must be smaller than the $SU(2)_L$ coupling constant g_L to avoid a too large $pp \to W' \to qq'$ cross section in conflict with limits from dijet and tb searches. In particular, the fit from Ref. [88] finds $\kappa \equiv g_R/g_L \sim 0.55 \ldots 0.7$ as the preferred region for $m_{W'} \sim 1.9$ TeV. Note that values $\kappa < 0.55$, while experimentally allowed, lead to a theoretical inconsistency in the model. At such small g_R, the model cannot reproduce the correct $U(1)_Y$ coupling $g_Y = (1/g_R^2 + 1/g_{B-L}^2)^{-1/2}$ after $SU(2)_R \times U(1)_{B-L}$ breaking. Of course, a scenario with $g_L \neq g_R$ may seem less aesthetic than one with $g_L = g_R$, but a difference between the two coupling constants is expected from renormalization group evolution [108, 109] and therefore does not prevent $SU(2)_L \times SU(2)_R \times U(1)_{B-L}$ from unifying into a larger gauge group at a higher scale.
- The W_L-W_R mixing angle should be of order $\sin\phi_w \sim 0.001 \ldots 0.002$ to give the

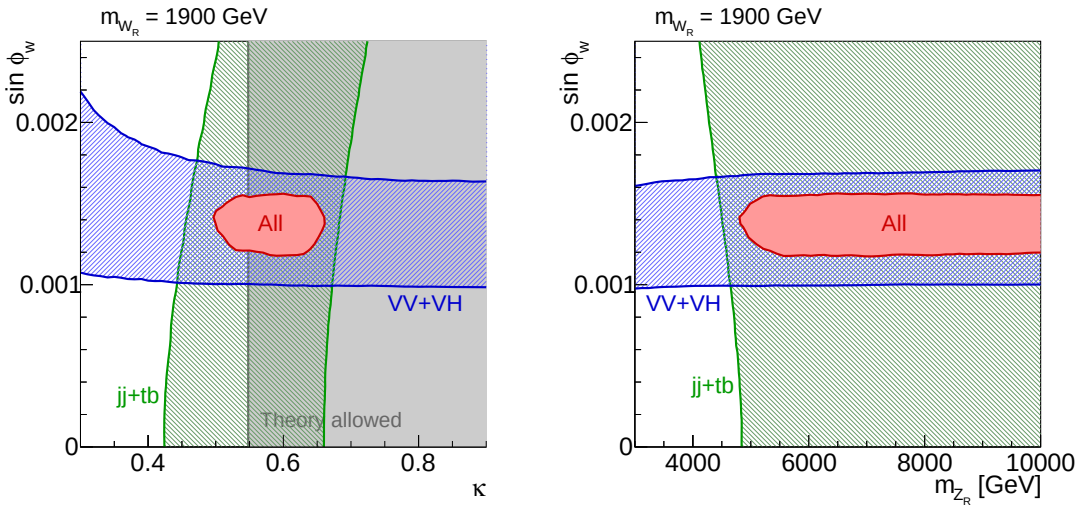


Figure 9: Preferred parameter region in the left-right symmetric model. This explanation of the diboson excess depends on only three parameters: the W' mass $m_{W'} \sim m_{W_R}$, the ratio $\kappa = g_R/g_L$ of the $SU(2)_L$ and $SU(2)_R$ gauge couplings, and the W_L-W_R mixing angle ϕ_w. In terms of these parameters, a lower limit on the Z_R mass can be derived (on the right). The blue (green) bands show the parameter regions in agreement with the diboson excess and Vh constraints (dijet and tb searches) at 68% CL. The region favoured by all searches combined is shown in red. Coupling constant ratios $\kappa < 0.55$ are forbidden by the condition that the breaking of $SU(2)_R \times U(1)_{B-L}$ to $U(1)_Y$ must yield the correct value for the hypercharge coupling constant. Figure taken from Ref. [88].

correct $W' \to WZ$ cross section [88].

These three parameters $m_{W'}$, κ, and ϕ_w not only determine the W' signal cross sections in the WZ, Wh, dijet, and tb final states, but also fix the Z' mass. Based on the experimental data, $m_{Z'}$ should be $\gtrsim$ few TeV (see the right panel of Fig. 9). Values much above the threshold are experimentally allowed, but require severe tuning of κ close to the theoretical limit 0.55.

It is worth mentioning that a left-right symmetric interpretation of the diboson excess can provide a few additional features:

- The left-right symmetric model might also allow an explanation of the CMS anomaly in the $eejj$ final state [11] with a $2.8\,\sigma$ significance. This excess can be interpreted as a signal of the decay $W' \to eN_R \to ee + (W'^* \to jj)$, where N_R is a heavy right-handed neutrino. Since CMS observe an excess only in opposite-sign electrons, while the data in the same-sign electron (and in the $\mu\mu jj$) channels are consistent with SM predictions, Refs. [86, 92, 95, 100] propose that at least one of the N_R is a pseudo-Dirac neutrino, thus suppressing the $e^{\pm}e^{\pm}jj$ final state compared to the $e^{\pm}e^{\mp}jj$ one.

- The model can be embedded in larger gauge groups such as an $SO(10)$ GUT [95, 103, 105] or in a non-commutative geometry framework [110].

- Possible connections between the left-right symmetric model and dark matter (DM) have been explored in the literature [88, 90]. These include (1) W'-mediated couplings between a right-handed neutrino DM candidate N and an SM charged lepton. This scenario can only work if N is lighter than the charged lepton it couples to, and if mixing with other right-handed neutrinos is absent to prevent DM decay. (2) A new $SU(2)_R$ multiplet. In this case, the DM candidate is accompanied by one or several new charged states potentially observable at the LHC. This scenario has the additional feature that the branching ratio of the W' boson to visible final states may be reduced, thus allowing for larger values of κ. (3) Supersymmetric dark matter. In supersymmetric left-right models, the lightest superpartner is an excellent DM candidate, in analogy to the MSSM.

3.3.2 Other models with extended gauge groups

While left-right symmetric scenarios have received the most attention in the context of the diboson anomaly, other classes of models are equally attractive. We begin by considering further scenarios in which the diboson anomaly is explained by a new charged gauge boson W' decaying to a WZ final state, or by a combination of approximately mass-degenerate W' and Z' bosons.

First, Refs. [85, 91] consider phenomenological models with a W' and a Z' boson, for instance based on the gauge group $SU(2)_L \times SU(2)_R \times U(1)_X$. Unlike in the scenarios discussed in the previous section, here the W' and Z' bosons can have equal masses and share responsibility for the observed excesses.

It is worth noting that "221 models" (models with gauge group $SU(2)\times SU(2)\times U(1)$) can also be interesting in contexts different from left-right symmetry [89, 111, 112]. For instance, different assignments of fermion quantum numbers can lead to scenarios in which the W' boson couples in a leptophobic, hadrophobic, fermiophobic, or flavor non-universal way. The authors of Ref. [111] consider the gauge group $SU(2) \times SU(2) \times U(1)$ in the context of a 3-site moose model in a deconstructed extra dimension, analysing both the scenario where only the W' boson is responsible for the diboson excess as well as the case with nearly mass-degenerate W' and Z' bosons around 2 TeV.

To supplement their study of 221 models, the authors of Ref. [89] have also considered a 331 model, i. e. a model in which the gauge group $SU(3)_c\times SU(3)_L\times U(1)_X$ is broken to the SM gauge group [113–115]. This leads to the emergence of five heavy gauge bosons: two pairs of charged bosons and one extra neutral boson that might be considered for the diboson excess. However, it turns out that this explanation is not favored by the data [89].

Very recently, the authors of Ref. [116] have considered a model with symmetry group $[SU(2)]^4 \times U(1)_{B-L}$, which preserves not only left-right symmetry, but also custodial symmetry. This effective theory is mainly motivated by strongly interacting models, but can also represent a weakly interacting extended gauge sector. It allows for an

explanation of the excess as a combination of two charged and two neutral gauge bosons at nearly the same mass, with the majority of the observed events coming from one of the charged bosons decaying as $W' \to WZ$ (see also Ref. [44]).

Since a clear discrimination between WZ, WW, and ZZ final states is currently not possible in a boosted diboson search, the ATLAS excess can also be explained in models with a Z' boson decaying to WW or ZZ. There is a sublety, though: it is difficult to achieve a sizable Z' coupling to ZZ states in simple models. On the other hand, an explanation of the ATLAS excess purely in terms of the decay $Z' \to (W \to jj) + (W \to jj)$ is in tension with strong constraints from searches for semileptonic final states, i. e. $Z' \to (W \to \ell\nu) + (W \to jj)$. Nevertheless, a plethora of explanations in terms of a Z' boson from an extra $U(1)$ group has been put forward [84, 117–122]. In most of these models the Z' boson is leptophobic to avoid the strong limits from $\ell^+\ell^-$ searches [84, 119–122].

Refs. [118–120] consider $U(1)'$ extensions of the SM motivated by string theory. The heavy Z' boson associated with this extra gauge factor can again be produced through a coupling to light quarks. In the model presented in Ref. [118], the cancellation of anomalies through the Green-Schwarz mechanism leads to a massive Z' boson with an effective coupling to two electroweak gauge bosons. This boson then decays not only into WW, but also to ZZ pairs, and can thus explain the diboson excess without violating semileptonic WW limits. At the same time, the effective coupling provides a $Z' \to Z\gamma$ decay. Such a signal is one of the hallmark predictions of this class of models.

3.4 Extended Higgs Sectors

There have been several attempts (*e.g.* [123–125]) to explain the observed diboson excess(es) as produced by ~ 2 TeV scalars originating in an extended Higgs sector, like a Two Higgs Doublet Model (2HDM). Here we discuss the generic features of such scenarios, and give a detailed overview of the problems they face in explaining the diboson excess. Before we go in the details of the models let us just emphasize several common features of these types of scenarios.

- The entire excess is coming from a neutral heavy Higgs boson, which is produced abundantly at the LHC and decays into ZZ and WW
- In order to have sufficient production cross sections, big couplings to the light quarks are introduced. Thus these scenarios are necessarily very far from MFV scenarios and they demand extremely severe fine-tuning in order to avoid abundant Falvor Changing Neutral Currents (FCNCs) in essentially almost all flavor measurements.
- In order not to be in direct conflict with the Higgs couplings measurements, the 2HDM must be in near alignment limit, which is in tension with getting large enough BRs into WW and ZZ.

Let us at this point focus for concreteness on a 2HDM scenario. This features two CP-even neutral scalars, h and H, the former being the 125 GeV Higgs particle while

the latter is considered as the 2 TeV particle responsible for the diboson excess via its decays $H \to WW, ZZ$. In order for H to have a sufficiently large production cross section, it needs to couple sizably to the first-generation quarks. On the other hand, a large coupling of the heavy Higgs boson to the first generation fermions will produce a large mass for the up or down quark, which would be unacceptable. In order to avoid this problem it is assumed that one doublet *does not develop a vev*, namely one parametrizes the Higgs doublets as follow:

$$H_1 = \begin{pmatrix} G^+ \\ \frac{v+\varphi_1+iG_0}{\sqrt{2}} \end{pmatrix} \qquad H_2 = \begin{pmatrix} H^+ \\ \frac{\varphi_2+iA_0}{\sqrt{2}} \end{pmatrix} \tag{7}$$

with H^+ and A_0 being respectively the physical charged and neutral CP-odd mass eigenstates, and G^+, G_0 being the Goldstone bosons. Namely we are in peculiar situation where $\tan\beta = \infty$, however the mixing angle between the CP even states α is different from $\pi/2$ or 0. This is in principle possible to achieve by carefully balancing the coefficients m_{12}^2 and λ_6 using the conventions of Ref. [126]. However, this situation is highly non-generic and also demands non-trivial fine-tuning.

In the *alignment limit* ($\cos(\beta-\alpha)=0$) of the 2HDM, $H_1 \equiv H_{\rm SM}$, and then $\varphi_1 = h$ is the SM Higgs boson. Away from this limit, the CP-even states φ_1 and φ_2 mix into the mass eigenstates $h = \sin(\beta-\alpha)\varphi_1 + \cos(\beta-\alpha)\varphi_2$, $H = -\cos(\beta-\alpha)\varphi_1 + \sin(\beta-\alpha)\varphi_2$. It is through this mixing that H can decay to WW and ZZ. Turning now to the Yukawa Lagrangian for the two scalar doublets $H_{1,2}$:

$$\mathcal{L}_Y = -\overline{Q}^i_L H_1\, y^i_d d^i_R - \overline{Q}^i_L (V^\dagger_{\rm CKM})^{ij} \tilde{H}_1\, y^j_u u^j_R - \overline{Q}^i_L H_2\, Y^{ij}_d d^j_R - \overline{Q}^i_L (V^\dagger_{\rm CKM})^{ij} \tilde{H}_2\, Y^{jk}_u u^k_R \tag{8}$$

where $Q = (V^\dagger_{\rm CKM} u_L, d_L)^T$ and the quarks are already written in the mass eigenbasis. The rationale in Refs. [123–125] is that, as H_2 does not develop a *vev*, and thus does not contribute to the quark masses, the couplings of H_2 to the first generation of quarks may be large, *e.g.* $Y_u^{11} = \sqrt{2} m_u/v \times \xi_u$, with $\xi_u \gg 1$. We however stress that generically $Y^{ij}_{u,d}$ in Eq. (8) would be 3×3 complex matrices with off-diagonal entries, leading to FCNCs mediated by H, and by virtue of the CP-even mixing, also by h. Even if $Y^{ij}_{u,d}$ would be (ad-hoc) taken to be diagonal at tree-level, this choice is not protected by any symmetry and would not be preserved by renormalization group evolution. This issue poses a serious threat to these models, but has not been analyzed in Refs. [123–125].

We now analyze the viability of such scenarios as an explanation of the diboson excess. First, due to the CP-even mixing, the light Higgs h will inherit the large H_2 couplings to first-generation quarks in (8), which may affect the Higgs signal strengths through an increase in Higgs production. The production cross section in $u\bar{u}$ initial states for h and H (at LO) is

$$\sigma(pp\,(u\bar{u}) \to h) \sim \left(\sqrt{2}\cos(\beta-\alpha)\,\xi_u\, m_u/v\right)^2 \times 54 \ \text{nb}, \tag{9}$$

$$\sigma(pp\,(u\bar{u}) \to H) \sim \left(\sqrt{2}\sin(\beta-\alpha)\,\xi_u\, m_u/v\right)^2 \times 0.52 \ \text{pb}. \tag{10}$$

For $m_u \sim 2.3$ MeV, $\xi_u \sim 10^4$ and $\cos(\beta-\alpha) \sim 0.01 - 0.1$ (as considered in Refs. [124, 125]), $\sigma(pp\,(u\bar{u}) \to h) \sim 0.1 - 10$ pb, to be compared to $\sigma(pp\,(gg) \to h) \sim 19.17$ pb in the SM (computed however at NNLO QCD and NLO EW). This sets an upper bound on the mixing parameter $\cos(\beta-\alpha)$ (as a function of ξ_u), and constitutes an important constraint on these models.

The necessary cross section to fit the diboson excess is $\sigma^H_{VV} \equiv \sigma(pp \to H) \times \mathrm{BR}(H \to WW, ZZ) \gtrsim 5$ fb. The relevant partial decays widths of H are

$$\Gamma_{H\to jj} \sim \frac{6\, m_u^2\, \xi_u^2\, m_H}{8\pi v^2} \qquad \Gamma_{H\to VV} \sim \frac{m_H^3}{16\pi v^2}\cos^2(\beta-\alpha) \qquad \Gamma_{H\to hh} \sim 9\,\Gamma_{H\to VV}. \quad (11)$$

The last relation follows from the equivalence theorem (see *e.g.* Ref. [127], and for more precise numerical estimates see Ref. [128]). The decay $H \to hh$ has however not been included in the analyses of [124, 125], and its inclusion will significantly affect the possibility of achieving the required σ^H_{VV}, particularly if $\Gamma_{H\to VV} \gg \Gamma_{H\to jj}$. As an example, Ref. [124] states that $\cos(\beta-\alpha) = 0.05$, $\xi_u = 0.8 \times 10^4$ yield $\sigma^H_{VV} \sim 5$ fb, while with the inclusion of $H \to hh$ and for fixed $\cos(\beta-\alpha) = 0.05$, the needed value for $\sigma^H_{VV} \sim 5$ fb is $\xi_u = 3.6 \times 10^4$, very close to the exclusion limit from dijet searches.

Another constraint to worry about has to do with the observed production cross sections and BRs of the observed Higgs boson. First of all, because in this model there are two states, which unitarize the WW scattering, the coupling of the SM-like Higgs boson to the vector bosons is modified by $r_V = \sin(\beta-\alpha)$. For $\cos(\beta-\alpha) \lesssim 0.1$ this leads to a very minor deviation of less than 1%. Similar deviations of $\sin(\beta-\alpha)$ are expected in couplings to the fermions if the matrices Y_u and Y_d are assumed to vanish. However, to have a large coupling between the heavy Higgs boson and the up-type quark we should at least assume that $(Y_u)^{uu} \sim 0.1$, triggering the new Higgs production mode according to Eq. (9). This coupling is virtually indistinguishable from the gluon couplings, and in the near alignment limit this is the only noticeable deviation of the Higgs couplings from the SM predictions. After LHC8 the measured deviation of the hgg coupling from the SM value is approximately $r_g \approx 0.87 \pm 0.2$ [129], such that deviations of order 30% are still allowed.

We finally comment on other possible spin-0 resonances as being responsible for the diboson excess. In Ref. [130] it has been demonstrated, concerning a diboson excess originating in the WZ final state, that $SU(2)_L$ singlet, charged spin-0 states cannot be responsible. Even though the arguments do not strictly apply to H^+ from the 2HDM, in this case the conclusions are similar as there exist no tree-level coupling $H^\pm W^\mp Z$.

4 Phenomenology for Run 2

We present here a discussion of how LHC Run 2 might determine the general properties of the diboson excesses near 2 TeV, under the assumption that they arise from fundamental (gauge or Higgs bosons) or composite states of new beyond the standard model intearctions. First we make some general remarks about production and decay modes of

resonances from each of the categories of models discussed in section 3. Then we propose several specific measurements that can help pin down the character of these interactions.

4.1 Resonance Production and Decay Modes

As discussed in Sect. 3, theoretical proposals for new physics responsible for the ATLAS and CMS 2 TeV excesses fall into a few broad categories:

1) New strong dynamics, involving heavy ρ and, possibly, a_1-like vector bosons associated with the 125 GeV Higgs boson H being a composite structure of some sort, e.g., Refs. [39–42, 44, 116].

2) Extended gauge dynamics, generally involving weakly-coupled heavy W' and/or Z' bosons; e.g., Refs. [85, 86, 88].

3) Extended Higgs-sector models, also generally involving weak coupling; see, e.g., Refs. [123–125]. Also see Refs. [75, 131] for spin-zero models inspired by strong dynamics.

4) Spin-two or effective operator frameworks that consider multiple spins.

The principal production mechanism at the LHC of the vector bosons of new strong or weak dynamics is the Drell-Yan (DY) process of $\bar{q}q'$ annihilation. For 2 TeV masses, their production rate at 13 TeV will be 5-7 times greater than at 8 TeV. In new strong dynamics, the vectors typically do not couple directly to standard model (SM) quarks and leptons, so their DY production proceeds via their mixing with γ, W, Z bosons. New weakly-coupled gauge bosons do couple directly to quarks and leptons. A secondary, but non-negligible production mechanism for these vector bosons, especially those associated with strong dynamics, is weak vector boson fusion (VBF), usually involving longitudinally-polarized W_L, Z_L bosons. The VBF rate of the vectors increases by an order of magnitude at 13 TeV. In the case of extended Higgs-sector models, the ATLAS/CMS diboson excesses are due to a neutral heavy Higgs boson, H'. Large couplings of this Higgs to first-generation quarks are assumed in order to explain the observed production rates. To accommodate this, H' must have no (appreciable) vacuum expectation value. Large light-quark couplings to H' may also lead to its production via gluon fusion (GGF).

In strong-dynamics models, there is an approximate isospin symmetry. In some models, there is also a left-right parity relating the masses and decay rates of the ρ and a-bosons. Then, the isotriplet ρ-bosons' main decay modes are *strong* decays into pairs of the Goldstone-boson pions which are the longitudinal weak bosons, i.e., $\rho^{\pm} \to W_L^{\pm} Z_L$ and $\rho^0 \to W_L^+ W_L^-$. These proceed through ρWW and ρWZ interactions whose strength is nominally $g_\rho M_W^2/M_\rho^2$, where g_ρ is a strong coupling, $\gtrsim \mathcal{O}(1)$. In some models, the ρ may also decay strongly into $W_L H$ and $Z_L H$. The isoscalar ω is likely to have nearly the same mass as the ρ, but it prefers to decay into $W_L^+ W_L^- Z_L$, a mode not yet sought at the LHC. The same is true of the $I = 1$ axial-vectors a, but there is a two-body

strong decay mode available to them, namely, $a^{\pm} \to W_L^{\pm} H$ and $a^0 \to Z_L H$. The coupling of the $a W_L H$ operators is nominally $g_\rho M_W$. In strong-dynamics models, the near degeneracy of ρ and a implied by the parity symmetry minimizes the contribution of the strong dynamics to the S-parameter [132, 133]. The parity also forbids $\rho \to V_L H$ and $a \to V_L V_L$ up to small electroweak corrections [116].

The coupling in the new weak gauge models is usually assumed to be of $\mathcal{O}(g)$, as for electroweak $SU(2)$. The W' and Z' bosons mix with their SM counterparts, W and Z, and this gives rise to $W'WZ$ and $Z'WW$ interactions which are nominally of order $gM_W^2/M_{W'}^2$. (A parity is at work here too.) The only appreciable decay of the heavy W', Z' to weak bosons is to $W_L^{\pm} Z_L$ and $W_L^+ W_L^-$. Note that neither the strong nor this weak scenario can produce copious ZZ signals. In these models, there often will be be $\ell^+\ell^-$ and $\ell^{\pm}\nu$ signals at rates comparable to the dibosons. The VH modes occur with a large branching fraction in the simplest LR models.

In 2HDM-inspired models, the VH and WZ signals come from other particles in the heavy Higgs doublet, either $A \to VH$ or $H^{\pm} \to WZ$, though the rates are usually larger than allowed by current data. Heavy H' resonances can also decay into HH, though this does not appear to have been considered. In Refs. [75, 131], the extended Higgs sector consists of a neutral particle only, so no WZ or VH modes are present. The scalar in this case is produced predominantly via GGF.

4.2 Proposed Run 2 Studies

Assuming that the ATLAS and CMS diboson excesses are confirmed in Run 2, understanding their nature will become a major program of these experiments. We present here a number of tests to determine whether their origin is strong or weak dynamics, their number and electric charges, and perhaps their spins and parities.

1) It is very desirable that the separation of $p_T \sim 1\,\text{TeV}$, nonleptonically-decaying W and Z bosons be sharpened, and the overlap between nonleptonic WW, WZ and ZZ selections be minimized. In W', Z' models and strong models with isovector resonances (ρ, a), there is no resonant ZZ production. In scalar or tensor models there are ZZ and WW resonances but, generally, very little WZ signal.

2) Determine the masses and individual cross sections for each nonleptonic diboson mode: $VV = WW$, WZ, ZZ.

3) Discover and measure the rates of the semileptonic modes of the VV excesses. These modes must be there if these are truly weak-boson resonances. Determine the ratios of semileptonic to nonleptonic rates as a check. In DY and VBF production of strong or weak vector bosons, $\sigma(\rho^+, W^{'+}) \simeq 3\sigma(\rho^-, W^{'-})$ and $\sigma(\rho^{\pm}, W^{'\pm}) \simeq 2\sigma(\rho^0, Z')$. With enough data, searches for 2-TeV resonant structure in all-leptonic modes will be possible.

4) Verify or exclude the presence of $VH = WH$, ZH modes in their semileptonic modes (e.g., $\ell^+\nu\bar{b}b$ and $\ell^+\ell^-\bar{b}b$, or leptons with $H \to \tau^+\tau^-$). Nonleptonic modes such as $J\bar{b}b$, where J is a fat V-jet should be sought as well.

5) If VH resonances exist, do they have the same mass as the VV resonances of the same electric charge? Determine individual VH cross sections and resonance branching ratios to VH.

6) Measure the resonance widths in each mode. These are an important discriminant between strong and weak-coupling dynamics as the source of the resonances. The W', Z' widths in weakly-coupled models scale as $g^2 M_{W',Z'}$ while the ρ, a widths in strongly-coupled models scale as $g_\rho^2 M_{\rho,a} \gg g^2 M_{W'}$.

7) Discriminate between longitudinally (V_L) and transversely (V_T) polarized weak bosons and determine their relative fractions in the VV and VH resonances. It has been suggested that nonleptonic V_L and V_T can be distinguished by the relative p_T of their decay subjets [134]. Will this be possible when $p_T(V) \sim 1\,\text{TeV}$? Also see Ref. [135].

8) The angular distribution of the fat jets and/or lepton pairs relative to the beam axis will help determine the spin of the VV and VH resonances. E.g., in Drell-Yan production of a heavy spin-one resonance, the resonance is almost at rest in the lab frame and it is polarized along the beam axis. Decays into $V_L V_L$ and $V_L H$ will have, approximately, a $\sin^2\theta$ distribution.

9) It will be useful to discriminate between production mechanisms: DY vs. VBF vs. GGF. In VBF there will be forward jets with moderate-p_T and a rapidity gap. Also GGF may be distinguished by the ratio of charged to neutral resonances. As just noted, DY production of spin-one should have distinctive angular distributions. The relative fraction of DY and VBF in a resonance's production may help determine its identity; see, e.g., Ref. [44]. The presence of extra jets may also indicate the production of multiple states or more complex decays, such as $W'' \to W'W \to 3W$ or $\omega \to W^+W^-Z$; see, e.g., [136].

10) Some models may have appreciable decay rates of the new resonances to dijets. E.g., the walking technicolor model [39] involves one family of technifermions and, therefore, color-octet ρ_T as well as singlets. The color-octet $\rho_T \to \bar{q}q$, gg modes may have large branching ratios because, in walking technicolor, their π_T-pair channels are closed kinematically. In extended gauge sector models and multi-Higgs models such as Ref. [86, 88, 123, 124] the 2-TeV resonance also has a significant branching fraction to dijets (either light flavor only, or both light and heavy flavor jets, i.e. $t\bar{b}$).

11) Many models predict additional bosonic resonances with masses in the few TeV range. Their masses and other properties are model-dependent. In some cases, it is possible that "partners" of the W' appear before the W' itself. An example is LR W' models, which predict a Z' slightly heavier than W' but which has a sizable branching fraction to $\ell^+\ell^-$, facilitating its earlier detection.

12) The presence or absence of top (and W, Z) partners can also distinguish between certain strong-interaction models and between strongly and weakly-coupled models. E.g., models in which H is a pseudo-Goldstone boson (see, e.g., Ref. [137, 138] for reviews) use such partners to stabilize the light Higgs mass, and they should show up soon at the LHC.

4.3 Precision Measurements

As explained in Section 3.4, models of the excesses involving extra Higgs bosons often predict sizable deviations from SM of the 125 GeV Higgs' couplings that may be observable at the LHC. Such deviations can be expected in some composite models with a spin-1 resonance decaying into electroweak bosons, particularly, but not always, models with moderately large values of the composite gauge self-coupling or with largely composite light quarks. (An exception to this is Ref. [139] in which the Higgs couplings deviate from SM by $\mathcal{O}(M_W^2/M_\rho^2)$.) The Higgs couplings are more SM-like in spin-zero and spin-two models. Although a detailed summary is beyond the scope of this report, some of those models give large contributions to FCNC's and/or violation of lepton flavor universality.

5 Overview of the Models

For the purpose of a condensed phenomenological overview of models addressing the diboson excess, in Table 1 we summarize the main production modes and decay channels of the particles responsible for the excesses in the different setups. We classify the models according to the nature of the relevant resonance(s), here spin and charges, and not according to the UV theory (which might be weakly or strongly coupled). Analyses not fitting in this simple format are listed under 'Unconventional'.

Spin-1 triplets ($V^{\pm}$, V^0)																
Prod.	WW	ZZ	WZ	Wh	Zh	γh	$W\gamma$	$Z\gamma$	$\gamma\gamma$	gg	hh	$\overline{Q}_3 Q_3$	$\bar{q}q$	ll	$\ell^{\pm}\nu$	X	Ref.
DY	✓		✓									(✓)	(✓)	(✓)	(✓)		[39, 140–142]
DY	✓		✓	✓	✓							$\checkmark_{\bar{q}q}$	✓	(✓)	(✓)		[40, 42, 43, 111]
DY	✓		✓	✓	✓							(✓)	(✓)	(✓)	(✓)		[44]
DY	✓		✓	✓	✓							$\checkmark_{\bar{q}q}$	✓	(✓)	(✓)	(✓)	[112]
DY	✓		✓	$\checkmark_{WZ}$	$\checkmark_{WW}$							$\checkmark_{\bar{q}q}$	✓	(✓)	(✓)		[45, 46, 85, 91]
DY	✓		✓	$\checkmark_{WZ}$	$\checkmark_{WW}$							✓	✓	(✓)	(✓)		[41]
Spin-1 V^0																
Prod.	WW	ZZ	WZ	Wh	Zh	γh	$W\gamma$	$Z\gamma$	$\gamma\gamma$	gg	hh	$\overline{Q}_3 Q_3$	$\bar{q}q$	ll	$\ell^{\pm}\nu$	X	Ref.
DY	✓				$\checkmark_{WW}$							$\checkmark_{\bar{q}q}$	✓				[84]
DY	✓				$\checkmark_{WW}$							$\checkmark_{\bar{q}q}$	✓	✓			[117]
DY	✓	✓						✓					✓				[118]
Spin-1 $V^{\pm}$																
Prod.	WW	ZZ	WZ	Wh	Zh	γh	$W\gamma$	$Z\gamma$	$\gamma\gamma$	gg	hh	$\overline{Q}_3 Q_3$	$\bar{q}q$	ll	$\ell^{\pm}\nu$	X	Ref.
DY			✓	$\checkmark_{WZ}$								$\checkmark_{\bar{q}q}$	✓			✓	[86, 90, 92–94]
DY			✓	$\checkmark_{WZ}$								$\checkmark_{\bar{q}q}$	✓				[87, 88]
Scalar																
Prod.	WW	ZZ	WZ	Wh	Zh	γh	$W\gamma$	$Z\gamma$	$\gamma\gamma$	gg	hh	$\overline{Q}_3 Q_3$	$\bar{q}q$	ll	$\ell^{\pm}\nu$	X	Ref.
gg	✓	✓						✓	✓	✓							[75, 131, 143]
gg	✓	✓						(✓)	(✓)	✓	$\checkmark_{WW/2}$	(✓)					[73]
gg	✓	$\checkmark_{WW/2}$				✓			✓	✓	✓	✓				(✓)	[141]
$q\bar{q}$	✓	$\checkmark_{WW/2}$		(✓)	(✓)						✓		✓			✓	[123–125]
'Unconventional'																
Torsion-free Einstein-Cartan theory																	[144]
Tri-boson interpretation: $pp \to R \to VY \to VV'X$																	[136]
[Implications in other observables (direct and indirect)]																	[95, 97, 142, 145–148]
[Next to leading order predictions]																	[148]
[Analysis techniques]																	[102, 106, 149, 150]

Table 1: Overview of the models. Checkmarks highlight relevant decay channels in the model at hand, while parentheses denote channels of subleading phenomenological importance. A subscript on the checkmark $\checkmark_f$ signals the branching ratio of the channel with final state f to be equal (to leading order) to the one considered in that column. We note that in some scenarios of the **Scalar** section, spin-2 resonance(s) could also be relevant for the excess (see e.g. [73]).

6 Conclusions

In this paper we have summarized the experimental situation of the alleged diboson excess around ~ 2 TeV seen by the LHC. We have provided a thorough analysis of the different channels with their relative significances. We have given different theoretical interpretations that necessarily imply the existence of new resonance(s) and an extension in the sector that breaks electroweak symmetry. All models fall into either supposing a strong coupling origin for the electroweak symmetry breaking or extending the gauge or Higgs sectors. We have given an overview of the different proposals and discussed the production cross section of the resonance capable of explaining the excess and its different decay modes. In the coming days the first results will be coming from the LHC run-II and we will get further hints to whether this is a real excess or just a statistical fluctuation.

Acknowledgements

We would like to heartily thank the organizers of the 2015 Les Houches workshop "Physics at TeV Colliders" where this work was initiated. J. B. is supported by the German Research Foundation (DFG) as part of GRK 1940 and FOR 2239. G.B. is supported by the National Science Foundation (grant NSF PHY-1404209). A.C. has been supported by a Marie Skłodowska-Curie Individual Fellowship of the European Commission's Horizon 2020 Programme under contract number 659239 NP4theLHC14. R.S.C., K.M., and E.H.S. are supported in part by the National Science Foundation under Grant Nos. PHY-0854889 and 1519045 to Michigan State University, as well as Grant No. PHY-1066293 to the Aspen Center for Physics. A.D.'s research is funded by the National Science Foundation (grant NSF PHY-1520966). F.G. acknowledges the support of a Marie Curie Intra European Fellowship within the EU FP7 (grant no. PIEF-GA-2013-628224). The work of J.L. Hewett and T.G. Rizzo was supported by the Department of Energy, Contract DE-AC02-76SF00515. The work of J.K. is supported by the German Research Foundation (DFG) under grant numbers FOR 2239 and KO 4820/1–1 and by the European Research Council (ERC) under the European Union's Horizon 2020 research and innovation programme (grant agreement No. 637506). K.L.'s research is supported in part by the U.S. Department of Energy under Grant No. DE-SC0010106. K.L. also gratefully acknowledges support of his Les Houches activities by the CERN Theory Group and by the Labex ENIGMASS of CNRS. The work of A.M. was partially supported by the National Science Foundation under Grant No. PHY-1417118. J.M.N. is supported by the People Programme (Marie curie Actions) of the European Union Seventh Framework Programme (FP7/2007-2013) under REA grant agreement PIEF-GA-2013-625809. A.O. is supported by grant MIURFIRB RBFR12H1MW. C.P. is supported by the UK Science and Technology Facilities Council (STFC) under grant ST/K001205/1. The work of M.Q. is partly supported by the Spanish Consolider-Ingenio 2010 Programme CPAN (CSD2007-00042), by MINECO under Grants CICYT-FEDER-FPA2011-25948 and CICYT-FEDER-FPA2014-55613-P, by the Severo Ochoa Excellence Program of MINECO under the grant SO-2012-0234, by Secretaria d'Universitats i Recerca del Departament d'Economia i Coneixement de la Generalitat de Catalunya under Grant 2014 SGR 1450, and by CNPq PVE fellowship project 405559/2013-5, Brazil. J.S. is supported by MINECO, under grant numbers FPA2010-17915 and FPA2013-47836-C3-2-P, by the European Commission through the contract PITN-GA-2012-316704 (HIGGSTOOLS) and by Junta de Andalucía grants FQM 101 and FQM 6552. V.S. is supported by the STFC. J. T. acknowledges support of the German Research Foundation (DFG) under grant number FOR 2239.

References

[1] F. Dias, S. Gadatsch, M. Gouzevich, C. Leonidopoulos, S. Novaes, A. Oliveira, M. Pierini, and T. Tomei, "Combination of Run-1 Exotic Searches in Diboson Final States at the LHC," 1512.03371.

[2] **ATLAS** Collaboration, "Search for high-mass diboson resonances with boson-tagged jets in proton-proton collisions at $\sqrt{s} = 8$ TeV with the ATLAS detector," 1506.00962.

[3] **CMS** Collaboration, "Search for massive resonances in dijet systems containing jets tagged as W or Z boson decays in pp collisions at $\sqrt{s} = 8$ TeV," *JHEP* **1408** (2014) 173, 1405.1994.

[4] **ATLAS** Collaboration, "Search for production of WW/WZ resonances decaying to a lepton, neutrino and jets in pp collisions at $\sqrt{s} = 8$ TeV with the ATLAS detector," *Eur.Phys.J.* **C75** (2015), no. 5, 209, 1503.04677.

[5] **CMS** Collaboration, "Search for massive resonances decaying into pairs of boosted bosons in semi-leptonic final states at $\sqrt{s} = 8$ TeV," *JHEP* **1408** (2014) 174, 1405.3447.

[6] **ATLAS** Collaboration, "Search for resonant diboson production in the $\ell\ell q\bar{q}$ final state in pp collisions at $\sqrt{s} = 8$ TeV with the ATLAS detector," *Eur.Phys.J.* **C75** (2015), no. 2, 69, 1409.6190.

[7] **ATLAS** Collaboration, "Search for a new resonance decaying to a W or Z boson and a Higgs boson in the $\ell\ell/\ell\nu/\nu\nu + b\bar{b}$ final states with the ATLAS Detector," 1503.08089.

[8] **CMS** Collaboration, "Search for massive WH resonances decaying to $\ell\nu\mathrm{b\bar{b}}$ final state in the boosted regime at $\sqrt{s} = 8\,\mathrm{TeV}$," Tech. Rep. CMS-PAS-EXO-14-010, CERN, Geneva, 2015.

[9] **CMS** Collaboration, "Search for a massive resonance decaying into a Higgs boson and a W or Z boson in hadronic final states in proton-proton collisions at sqrt(s) = 8 TeV," 1506.01443.

[10] **CMS** Collaboration, "Search for narrow high-mass resonances in proton-proton collisions at $\sqrt{s} = 8$ TeV decaying to Z and Higgs bosons," 1502.04994.

[11] **CMS** Collaboration, "Search for heavy neutrinos and W bosons with right-handed couplings in proton-proton collisions at $\sqrt{s} = 8\,\mathrm{TeV}$," *Eur.Phys.J.* **C74** (2014), no. 11, 3149, 1407.3683.

[12] **ATLAS** Collaboration, "Search for new phenomena in the dijet mass distribution using $p - p$ collision data at $\sqrt{s} = 8$ TeV with the ATLAS detector," *Phys.Rev.* **D91** (2015), no. 5, 052007, 1407.1376.

[13] **CMS** Collaboration, "Search for resonances and quantum black holes using dijet mass spectra in proton-proton collisions at $\sqrt{s} = 8$ TeV," *Phys.Rev.* **D91** (2015), no. 5, 052009, 1501.04198.

[14] **ATLAS** Collaboration, "Search for high-mass dilepton resonances in pp collisions at $\sqrt{s} = 8$ TeV with the ATLAS detector," *Phys.Rev.* **D90** (2014), no. 5, 052005, 1405.4123.

[15] **CMS** Collaboration, "Search for heavy narrow dilepton resonances in *pp* collisions at $\sqrt{s} = 7$ TeV and $\sqrt{s} = 8$ TeV," *Phys.Lett.* **B720** (2013) 63–82, 1212.6175.

[16] **ATLAS** Collaboration, "Expected Performance of the ATLAS Experiment - Detector, Trigger and Physics," 0901.0512.

[17] R. M. Harris and K. Kousouris, "Searches for Dijet Resonances at Hadron Colliders," *Int. J. Mod. Phys.* **A26** (2011) 5005–5055, 1110.5302.

[18] **Particle Data Group** Collaboration, K. A. Olive *et. al.*, "Review of Particle Physics," *Chin. Phys.* **C38** (2014) 090001.

[19] J. Pumplin, D. R. Stump, J. Huston, H. L. Lai, P. M. Nadolsky, and W. K. Tung, "New generation of parton distributions with uncertainties from global QCD analysis," *JHEP* **07** (2002) 012, hep-ph/0201195.

[20] R. S. Chivukula, K. Mohan, and E. H. Simmons, "Simplified Limits (in preparation)," Tech. Rep. MSUHEP-1601xx, 2016.

[21] S. Dawson, "The Effective W Approximation," *Nucl. Phys.* **B249** (1985) 42–60.

[22] S. Weinberg, "Implications of Dynamical Symmetry Breaking: An Addendum," *Phys. Rev.* **D19** (1979) 1277–1280.

[23] L. Susskind, "Dynamics of Spontaneous Symmetry Breaking in the Weinberg-Salam Theory," *Phys. Rev.* **D20** (1979) 2619–2625.

[24] S. Dimopoulos and J. Preskill, "Massless Composites With Massive Constituents," *Nucl. Phys.* **B199** (1982) 206.

[25] D. B. Kaplan and H. Georgi, "SU(2) x U(1) Breaking by Vacuum Misalignment," *Phys. Lett.* **B136** (1984) 183.

[26] D. B. Kaplan, H. Georgi, and S. Dimopoulos, "Composite Higgs Scalars," *Phys. Lett.* **B136** (1984) 187.

[27] H. Georgi, D. B. Kaplan, and P. Galison, "Calculation of the Composite Higgs Mass," *Phys. Lett.* **B143** (1984) 152.

[28] H. Georgi and D. B. Kaplan, "Composite Higgs and Custodial SU(2)," *Phys. Lett.* **B145** (1984) 216.

[29] M. J. Dugan, H. Georgi, and D. B. Kaplan, "Anatomy of a Composite Higgs Model," *Nucl. Phys.* **B254** (1985) 299.

[30] R. Contino, Y. Nomura, and A. Pomarol, "Higgs as a holographic pseudoGoldstone boson," *Nucl. Phys.* **B671** (2003) 148–174, hep-ph/0306259.

[31] K. Agashe, R. Contino, and A. Pomarol, "The Minimal composite Higgs model," *Nucl. Phys.* **B719** (2005) 165–187, hep-ph/0412089.

[32] R. Contino, "The Higgs as a Composite Nambu-Goldstone Boson," in *Physics of the large and the small, TASI 09, proceedings of the Theoretical Advanced Study Institute in Elementary Particle Physics, Boulder, Colorado, USA, 1-26 June 2009*, pp. 235–306. 2011. 1005.4269.

[33] G. V. Dzhikiya, "The dilaton as the analog of the Higgs boson in composite models," *Sov. J. Nucl. Phys.* **45** (1987) 1083–1087. [Yad. Fiz.45,1750(1987)].

[34] T. Appelquist and Y. Bai, "A Light Dilaton in Walking Gauge Theories," *Phys. Rev.* **D82** (2010) 071701, 1006.4375.

[35] B. Grinstein and P. Uttayarat, "A Very Light Dilaton," *JHEP* **07** (2011) 038, 1105.2370.

[36] S. Matsuzaki and K. Yamawaki, "Techni-dilaton at 125 GeV," *Phys. Rev.* **D85** (2012) 095020, 1201.4722.

[37] B. Bellazzini, C. Csaki, J. Hubisz, J. Serra, and J. Terning, "A Higgslike Dilaton," *Eur. Phys. J.* **C73** (2013), no. 2, 2333, 1209.3299.

[38] R. L. Altmeyer, M. Gockeler, R. Horsley, E. Laermann, G. Schierholz, and P. M. Zerwas, "Hadronic coupling constants in lattice QCD," *Z. Phys.* **C68** (1995) 443–450, hep-lat/9504003.

[39] H. S. Fukano, M. Kurachi, S. Matsuzaki, K. Terashi, and K. Yamawaki, "2 TeV Walking Technirho at LHC?," *Phys. Lett.* **B750** (2015) 259–265, 1506.03751.

[40] D. B. Franzosi, M. T. Frandsen, and F. Sannino, "Diboson Signals via Fermi Scale Spin-One States," 1506.04392.

[41] A. Thamm, R. Torre, and A. Wulzer, "Composite Heavy Vector Triplet in the ATLAS Diboson Excess," *Phys. Rev. Lett.* **115** (2015), no. 22, 221802, 1506.08688.

[42] A. Carmona, A. Delgado, M. Quiros, and J. Santiago, "Diboson resonant production in non-custodial composite Higgs models," *JHEP* **09** (2015) 186, 1507.01914.

[43] L. Bian, D. Liu, and J. Shu, "Low Scale Composite Higgs Model and 1.8 $\sim$ 2 TeV Diboson Excess," 1507.06018.

[44] K. Lane and L. Pritchett, "Heavy Vector Partners of the Light Composite Higgs," 1507.07102.

[45] M. Low, A. Tesi, and L.-T. Wang, "Composite spin-1 resonances at the LHC," *Phys. Rev.* **D92** (2015), no. 8, 085019, 1507.07557.

[46] C. Niehoff, P. Stangl, and D. M. Straub, "Direct and indirect signals of natural composite Higgs models," 1508.00569.

[47] M. Baak, M. Goebel, J. Haller, A. Hoecker, D. Kennedy, R. Kogler, K. Moenig, M. Schott, and J. Stelzer, "The Electroweak Fit of the Standard Model after the Discovery of a New Boson at the LHC," *Eur. Phys. J.* **C72** (2012) 2205, 1209.2716.

[48] D. Marzocca, M. Serone, and J. Shu, "General Composite Higgs Models," *JHEP* **08** (2012) 013, 1205.0770.

[49] T. Appelquist and F. Sannino, "The Physical spectrum of conformal SU(N) gauge theories," *Phys. Rev.* **D59** (1999) 067702, hep-ph/9806409.

[50] T. Appelquist, P. S. Rodrigues da Silva, and F. Sannino, "Enhanced global symmetries and the chiral phase transition," *Phys. Rev.* **D60** (1999) 116007, hep-ph/9906555.

[51] J. Hirn and V. Sanz, "A Negative S parameter from holographic technicolor," *Phys. Rev. Lett.* **97** (2006) 121803, hep-ph/0606086.

[52] J. Hirn and V. Sanz, "The Fifth dimension as an analogue computer for strong interactions at the LHC," *JHEP* **03** (2007) 100, hep-ph/0612239.

[53] R. Foadi, M. T. Frandsen, T. A. Ryttov, and F. Sannino, "Minimal Walking Technicolor: Set Up for Collider Physics," *Phys. Rev.* **D76** (2007) 055005, 0706.1696.

[54] R. Contino, L. Da Rold, and A. Pomarol, "Light custodians in natural composite Higgs models," *Phys. Rev.* **D75** (2007) 055014, hep-ph/0612048.

[55] A. D. Medina, N. R. Shah, and C. E. M. Wagner, "Gauge-Higgs Unification and Radiative Electroweak Symmetry Breaking in Warped Extra Dimensions," *Phys. Rev.* **D76** (2007) 095010, 0706.1281.

[56] C. Csaki, A. Falkowski, and A. Weiler, "The Flavor of the Composite Pseudo-Goldstone Higgs," *JHEP* **09** (2008) 008, 0804.1954.

[57] O. Matsedonskyi, G. Panico, and A. Wulzer, "Light Top Partners for a Light Composite Higgs," *JHEP* **01** (2013) 164, 1204.6333.

[58] A. Pomarol and F. Riva, "The Composite Higgs and Light Resonance Connection," *JHEP* **08** (2012) 135, 1205.6434.

[59] C. Anastasiou, E. Furlan, and J. Santiago, "Realistic Composite Higgs Models," *Phys. Rev.* **D79** (2009) 075003, 0901.2117.

[60] J. A. Cabrer, G. von Gersdorff, and M. Quiros, "Suppressing Electroweak Precision Observables in 5D Warped Models," *JHEP* **05** (2011) 083, 1103.1388.

[61] A. Carmona, E. Ponton, and J. Santiago, "Phenomenology of Non-Custodial Warped Models," *JHEP* **10** (2011) 137, 1107.1500.

[62] R. Contino and M. Salvarezza, "One-loop effects from spin-1 resonances in Composite Higgs models," *JHEP* **07** (2015) 065, 1504.02750.

[63] K. Agashe, S. Gopalakrishna, T. Han, G.-Y. Huang, and A. Soni, "LHC Signals for Warped Electroweak Charged Gauge Bosons," *Phys. Rev.* **D80** (2009) 075007, 0810.1497.

[64] D. Barducci, A. Belyaev, S. De Curtis, S. Moretti, and G. M. Pruna, "Exploring Drell-Yan signals from the 4D Composite Higgs Model at the LHC," *JHEP* **04** (2013) 152, 1210.2927.

[65] N. Vignaroli, "New W$'$ signals at the LHC," *Phys. Rev.* **D89** (2014), no. 9, 095027, 1404.5558.

[66] D. Greco and D. Liu, "Hunting composite vector resonances at the LHC: naturalness facing data," *JHEP* **12** (2014) 126, 1410.2883.

[67] G. Panico, M. Redi, A. Tesi, and A. Wulzer, "On the Tuning and the Mass of the Composite Higgs," *JHEP* **03** (2013) 051, 1210.7114.

[68] A. Carmona and F. Goertz, "A naturally light Higgs without light Top Partners," *JHEP* **05** (2015) 002, 1410.8555.

[69] M. Geller and O. Telem, "Holographic Twin Higgs Model," *Phys. Rev. Lett.* **114** (2015) 191801, 1411.2974.

[70] R. Barbieri, D. Greco, R. Rattazzi, and A. Wulzer, "The Composite Twin Higgs scenario," *JHEP* **08** (2015) 161, 1501.07803.

[71] M. Low, A. Tesi, and L.-T. Wang, "Twin Higgs mechanism and a composite Higgs boson," *Phys. Rev.* **D91** (2015) 095012, 1501.07890.

[72] V. Sanz and J. Setford, "Composite Higgses with seesaw EWSB," *JHEP* **XX** (2015) XXX, 1508.06133.

[73] V. Sanz, "On the compatibility of the diboson excess with a gg-initiated composite sector," 1507.03553.

[74] M. J. Teper, "Glueball masses and other physical properties of SU(N) gauge theories in D = (3+1): A Review of lattice results for theorists," hep-th/9812187.

[75] C.-W. Chiang, H. Fukuda, K. Harigaya, M. Ibe, and T. T. Yanagida, "Diboson Resonance as a Portal to Hidden Strong Dynamics," *JHEP* **11** (2015) 015, 1507.02483.

[76] M. S. Chanowitz and M. K. Gaillard, "The TeV Physics of Strongly Interacting W's and Z's," *Nucl. Phys.* **B261** (1985) 379.

[77] J. C. Pati and A. Salam, "LEPTON NUMBER AS THE FOURTH COLOR," *Phys. Rev.* **D10** (1974) 275–289.

[78] R. N. Mohapatra and J. C. Pati, "Left-Right Gauge Symmetry and an Isoconjugate Model of CP Violation," *Phys. Rev.* **D11** (1975) 566–571.

[79] R. N. Mohapatra and J. C. Pati, "A Natural Left-Right Symmetry," *Phys. Rev.* **D11** (1975) 2558.

[80] G. Senjanovic and R. N. Mohapatra, "Exact Left-Right Symmetry and Spontaneous Violation of Parity," *Phys. Rev.* **D12** (1975) 1502.

[81] R. N. Mohapatra, *UNIFICATION AND SUPERSYMMETRY. THE FRONTIERS OF QUARK - LEPTON PHYSICS*. Springer, Berlin, 1986.

[82] N. G. Deshpande, J. F. Gunion, B. Kayser, and F. I. Olness, "Left-right symmetric electroweak models with triplet Higgs," *Phys. Rev.* **D44** (1991) 837–858.

[83] M. Dhuria, C. Hati, R. Rangarajan, and U. Sarkar, "Falsifying leptogenesis for a TeV scale $W_R^{\pm}$ at the LHC," *Phys. Rev.* **D92** (2015), no. 3, 031701, 1503.07198.

[84] J. Hisano, N. Nagata, and Y. Omura, "Interpretations of the ATLAS Diboson Resonances," *Phys. Rev.* **D92** (2015), no. 5, 055001, 1506.03931.

[85] K. Cheung, W.-Y. Keung, P.-Y. Tseng, and T.-C. Yuan, "Interpretations of the ATLAS Diboson Anomaly," *Phys. Lett.* **B751** (2015) 188–194, 1506.06064.

[86] B. A. Dobrescu and Z. Liu, "W′ Boson near 2 TeV: Predictions for Run 2 of the LHC," *Phys. Rev. Lett.* **115** (2015), no. 21, 211802, 1506.06736.

[87] Y. Gao, T. Ghosh, K. Sinha, and J.-H. Yu, "SU(2)×SU(2)×U(1) interpretations of the diboson and Wh excesses," *Phys. Rev.* **D92** (2015), no. 5, 055030, 1506.07511.

[88] J. Brehmer, J. Hewett, J. Kopp, T. Rizzo, and J. Tattersall, "Symmetry Restored in Dibosons at the LHC?," *JHEP* **10** (2015) 182, 1507.00013.

[89] Q.-H. Cao, B. Yan, and D.-M. Zhang, "Simple non-Abelian extensions of the standard model gauge group and the diboson excesses at the LHC," *Phys. Rev.* **D92** (2015), no. 9, 095025, 1507.00268.

[90] J. Heeck and S. Patra, "Minimal Left-Right Symmetric Dark Matter," *Phys. Rev. Lett.* **115** (2015), no. 12, 121804, 1507.01584.

[91] B. C. Allanach, B. Gripaios, and D. Sutherland, "Anatomy of the ATLAS diboson anomaly," *Phys. Rev.* **D92** (2015), no. 5, 055003, 1507.01638.

[92] B. A. Dobrescu and Z. Liu, "Heavy Higgs bosons and the 2 TeV W$'$ boson," *JHEP* **10** (2015) 118, 1507.01923.

[93] P. S. Bhupal Dev and R. N. Mohapatra, "Unified explanation of the $eejj$, diboson and dijet resonances at the LHC," *Phys. Rev. Lett.* **115** (2015), no. 18, 181803, 1508.02277.

[94] P. Coloma, B. A. Dobrescu, and J. Lopez-Pavon, "Right-Handed Neutrinos and the 2 TeV W' Boson," 1508.04129.

[95] F. F. Deppisch, L. Graf, S. Kulkarni, S. Patra, W. Rodejohann, N. Sahu, and U. Sarkar, "Reconciling the 2 TeV Excesses at the LHC in a Linear Seesaw Left-Right Model," 1508.05940.

[96] T. Bandyopadhyay, B. Brahmachari, and A. Raychaudhuri, "Implications of the CMS search for W_R on Grand Unification," 1509.03232.

[97] R. L. Awasthi, P. S. B. Dev, and M. Mitra, "Implications of the Diboson Excess for Neutrinoless Double Beta Decay and Lepton Flavor Violation in TeV Scale Left Right Symmetric Model," 1509.05387.

[98] P. Ko and T. Nomura, "SU(2)$_L\times$SU(2)$_R$ minimal dark matter with 2 TeV W'," 1510.07872.

[99] J. H. Collins and W. H. Ng, "A 2 TeV W_R, Supersymmetry, and the Higgs Mass," 1510.08083.

[100] B. A. Dobrescu and P. J. Fox, "Signals of a 2 TeV W' boson and a heavier Z' boson," 1511.02148.

[101] K. Das, T. Li, S. Nandi, and S. K. Rai, "The Diboson Excesses in an Anomaly Free Leptophobic Left-Right Model," 1512.00190.

[102] J. A. Aguilar-Saavedra and J. Bernabeu, "Breaking down the entire W boson spin observables from its decay," 1508.04592.

[103] G. Bambhaniya, P. S. B. Dev, S. Goswami, and M. Mitra, "The Scalar Triplet Contribution to Lepton Flavour Violation and Neutrinoless Double Beta Decay in Left-Right Symmetric Model," 1512.00440.

[104] M. Hirsch, M. E. Krauss, T. Opferkuch, W. Porod, and F. Staub, "A constrained supersymmetric left-right model," 1512.00472.

[105] U. Aydemir, "SO(10) Grand Unification in light of recent LHC searches and colored scalars at the TeV-scale," 1512.00568.

[106] L. Bian, D. Liu, J. Shu, and Y. Zhang, "Interference Effect on Resonance Studies and the Diboson Excess," 1509.02787.

[107] J. A. Aguilar-Saavedra and F. R. Joaquim, "Multiboson production in W' decays," 1512.00396.

[108] T. G. Rizzo and G. Senjanovic, "Grand Unification and Parity Restoration at Low-energies. 2. Unification Constraints," *Phys. Rev.* **D25** (1982) 235.

[109] D. Chang, R. N. Mohapatra, and M. K. Parida, "Decoupling Parity and SU(2)-R Breaking Scales: A New Approach to Left-Right Symmetric Models," *Phys. Rev. Lett.* **52** (1984) 1072.

[110] U. Aydemir, D. Minic, C. Sun, and T. Takeuchi, "Pati-Salam Unification from Non-commutative Geometry and the TeV-scale W_R boson," 1509.01606.

[111] T. Abe, R. Nagai, S. Okawa, and M. Tanabashi, "Unitarity sum rules, three-site moose model, and the ATLAS 2 TeV diboson anomalies," *Phys. Rev.* **D92** (2015), no. 5, 055016, 1507.01185.

[112] T. Abe, T. Kitahara, and M. M. Nojiri, "Prospects for Spin-1 Resonance Search at 13 TeV LHC and the ATLAS Diboson Excess," 1507.01681.

[113] F. Pisano and V. Pleitez, "An SU(3) x U(1) model for electroweak interactions," *Phys. Rev.* **D46** (1992) 410–417, hep-ph/9206242.

[114] R. Foot, O. F. Hernandez, F. Pisano, and V. Pleitez, "Lepton masses in an SU(3)-L x U(1)-N gauge model," *Phys. Rev.* **D47** (1993) 4158–4161, hep-ph/9207264.

[115] P. H. Frampton, "Chiral dilepton model and the flavor question," *Phys. Rev. Lett.* **69** (1992) 2889–2891.

[116] T. Appelquist, Y. Bai, J. Ingoldby, and M. Piai, "Spectrum-doubled Heavy Vector Bosons at the LHC," 1511.05473.

[117] A. Alves, A. Berlin, S. Profumo, and F. S. Queiroz, "Dirac-fermionic dark matter in $U(1)_X$ models," *JHEP* **10** (2015) 076, 1506.06767.

[118] L. A. Anchordoqui, I. Antoniadis, H. Goldberg, X. Huang, D. Lust, and T. R. Taylor, "Stringy origin of diboson and dijet excesses at the LHC," *Phys. Lett.* **B749** (2015) 484–488, 1507.05299.

[119] A. E. Faraggi and M. Guzzi, "Extra Z' s and W' s in heterotic-string derived models," *Eur. Phys. J.* **C75** (2015), no. 11, 537, 1507.07406.

[120] T. Li, J. A. Maxin, V. E. Mayes, and D. V. Nanopoulos, "The Diboson Excesses in Leptophobic $U(1)_{\rm LP}$ Models from String Theories," 1509.06821.

[121] Z.-W. Wang, F. S. Sage, T. G. Steele, and R. B. Mann, "Can an Asymptotically-Safe Conformal $U(1)'$ Model Address the LHC Diboson Excess?," 1511.02531.

[122] W.-Z. Feng, Z. Liu, and P. Nath, "ATLAS Diboson Excess from Stueckelberg Mechanism," 1511.08921.

[123] C.-H. Chen and T. Nomura, "2 TeV Higgs boson and diboson excess at the LHC," *Phys. Lett.* **B749** (2015) 464–468, 1507.04431.

[124] Y. Omura, K. Tobe, and K. Tsumura, "Survey of Higgs interpretations of the diboson excesses," *Phys. Rev.* **D92** (2015), no. 5, 055015, 1507.05028.

[125] W. Chao, "ATLAS Diboson Excesses from the Stealth Doublet Model," 1507.05310.

[126] J. F. Gunion and H. E. Haber, "The CP conserving two Higgs doublet model: The Approach to the decoupling limit," *Phys. Rev.* **D67** (2003) 075019, hep-ph/0207010.

[127] A. Katz, M. Reece, and A. Sajjad, "Naturalness, $b \to s\gamma$, and SUSY heavy Higgses," *JHEP* **10** (2014) 102, 1406.1172.

[128] N. Craig, J. Galloway, and S. Thomas, "Searching for Signs of the Second Higgs Doublet," 1305.2424.

[129] P. P. Giardino, K. Kannike, I. Masina, M. Raidal, and A. Strumia, "The universal Higgs fit," *JHEP* **05** (2014) 046, 1303.3570.

[130] A. Sajjad, "Understanding diboson anomalies," 1511.02244.

[131] G. Cacciapaglia, A. Deandrea, and M. Hashimoto, "Scalar Hint from the Diboson Excess?," *Phys. Rev. Lett.* **115** (2015), no. 17, 171802, 1507.03098.

[132] R. Casalbuoni *et. al.*, "Degenerate BESS Model: The possibility of a low energy strong electroweak sector," *Phys. Rev.* **D53** (1996) 5201–5221, hep-ph/9510431.

[133] K. Lane and A. Martin, "An Effective Lagrangian for Low-Scale Technicolor," *Phys. Rev.* **D80** (2009) 115001, 0907.3737.

[134] Y. Cui, Z. Han, and M. D. Schwartz, "W-jet Tagging: Optimizing the Identification of Boosted Hadronically-Decaying W Bosons," *Phys. Rev.* **D83** (2011) 074023, 1012.2077.

[135] **CMS** Collaboration, "Identification techniques for highly boosted W bosons that decay into hadrons," *JHEP* **1412** (2014) 017, 1410.4227.

[136] J. A. Aguilar-Saavedra, "Triboson interpretations of the ATLAS diboson excess," *JHEP* **10** (2015) 099, 1506.06739.

[137] B. Bellazzini, C. Csáki, and J. Serra, "Composite Higgses," *Eur.Phys.J.* **C74** (2014), no. 5, 2766, 1401.2457.

[138] G. Panico and A. Wulzer, "The Composite Nambu-Goldstone Higgs," 1506.01961.

[139] K. Lane, "A composite Higgs model with minimal fine-tuning: The large-N and weak-technicolor limit," *Phys. Rev.* **D90** (2014), no. 9, 095025, 1407.2270.

[140] G. Cacciapaglia and M. T. Frandsen, "Unitarity implications of a diboson resonance in the TeV region for Higgs physics," *Phys. Rev.* **D92** (2015) 055035, 1507.00900.

[141] H. Terazawa and M. Yasue, "Excited Gauge and Higgs Bosons in the Unified Composite Model," 1508.00172.

[142] A. Dobado, F.-K. Guo, and F. J. Llanes-Estrada, "Production cross section estimates for strongly-interacting Electroweak Symmetry Breaking Sector resonances at particle colliders," *Commun. Theor. Phys.* **64** (2015) 701–709, 1508.03544.

[143] C. Petersson and R. Torre, "ATLAS diboson excess from low scale supersymmetry breaking," 1508.05632.

[144] S.-S. Xue, "Vector-like $W^{\pm}$-boson coupling at TeV and fermion-mass hierarchy (two boson-tagged jets vs four quark jets)," 1506.05994.

[145] H. S. Fukano, S. Matsuzaki, and K. Yamawaki, "Conformal Barrier for New Vector Bosons Decay to the Higgs," 1507.03428.

[146] S. P. Liew and S. Shirai, "Testing ATLAS Diboson Excess with Dark Matter Searches at LHC," 1507.08273.

[147] P. Arnan, D. Espriu, and F. Mescia, "Interpreting a 2 TeV resonance in WW scattering," 1508.00174.

[148] T. Ježo, M. Klasen, D. R. Lamprea, F. Lyonnet, and I. Schienbein, "NLO+NLL limits on W' and Z' gauge boson masses," 2015. 1508.03539.

[149] D. Gonçalves, F. Krauss, and M. Spannowsky, "Augmenting the diboson excess for the LHC Run II," *Phys. Rev.* **D92** (2015), no. 5, 053010, 1508.04162.

[150] F. J. Llanes-Estrada, A. Dobado, and R. L. Delgado, "Describing 2-TeV scale W_LW_L resonances with Unitarized Effective Theory," in *18th Workshop on What Comes Beyond the Standard Models? Bled, Slovenia, July 11-19, 2015.* 2015. 1509.00441.